Available online at www.CivileJournal.org

Civil Engineering Journal

(E-ISSN: 2476-3055; ISSN: 2676-6957)

Vol. 12, No. 01, January, 2026

Evaluation of Fresh Properties of Cement Pastes: Part II-Modelling via Central Composite Design

Lino Maia [1*]

[1] *CONSTRUCT, Faculdade de Engenharia (FEUP), Universidade do Porto, Rua Dr. Roberto Frias, 4200-465 Porto, Portugal.*

Received 28 July 2025; Revised 11 December 2025; Accepted 19 December 2025; Published 01 January 2026

Abstract

This study investigates how variations in constituent materials affect the fresh properties of cement-based pastes using a statistically driven experimental approach. A Central Composite Design (CCD) was implemented to examine the influence of three key input parameters: water-to-cement ratio (w/c), superplasticizer-to-powder ratio (Sp/p), and water-to-powder ratio (w/p). Fifteen mix compositions were produced and tested using the mini-slump test and Marsh funnel flow time, both immediately after mixing and after 60 minutes. Response Surface Methodology (RSM) was applied to develop predictive models for each property. The results showed that the water-to-powder ratio was the most influential factor on workability, followed by the superplasticizer-to-powder ratio. The statistical models successfully captured main, interaction, and quadratic effects, enabling accurate prediction of flow and time measurements. These models were further used to optimize mix compositions according to targeted fresh-state performance. Compared with conventional one-variable-at-a-time approaches, the CCD method substantially reduces the number of tests required while providing deeper analytical insights. The proposed methodology improves the understanding of complex interactions among mix parameters and supports the efficient design of cement-based materials for performance-critical applications.

Keywords: Cement Paste; Central Composite Design; Modelling; Statistical Approach.

1. Introduction

The evaluation of fresh-state properties of cement-based pastes is a critical step in ensuring proper workability, pumpability, and structural build-up of modern cementitious materials. Fresh properties such as flowability, yield stress, viscosity, and setting behavior directly influence casting quality, dimensional stability, and ultimately hardened performance. This is particularly relevant for advanced applications such as self-compacting concrete (SCC), ultra-high-performance concrete (UHPC), 3D-printed concretes, and other innovative cementitious systems [1–3]. Even minor changes in binder composition, water-to-cement ratio (w/c), or superplasticizer dosage can significantly alter rheological responses, underlining the need for systematic evaluation [4–6].

Two main lines of research have been developed. The first focuses on the role of constituent materials in modifying fresh properties. Studies show that mineral additions, filler type, and chemical admixtures can strongly affect slump flow, viscosity, and setting [7–9]. Recent contributions also highlight the impact of supplementary cementitious materials and sustainable binders [10, 11]. The second line of research is the use of advanced experimental design strategies to optimize mixes while reducing testing effort. Approaches such as factorial design, Taguchi arrays, Box–Behnken design, response surface methodology (RSM), and hybrid methods integrating artificial intelligence have been increasingly applied [12–15].

* Corresponding author: linomaia@fe.up.pt

https://doi.org/10.28991/CEJ-2026-012-01-03

Despite progress, significant knowledge gaps remain. Most optimization-oriented studies emphasize hardened properties such as compressive strength and durability while devoting limited attention to early-age rheology [16–18]. Some works applying RSM or CCD to SCC or UHPC focused primarily on strength, neglecting fresh-state interactions [19–21]. When rheological behavior is considered, many investigations rely on one-variable-at-a-time methods, which are resource-intensive and unable to capture nonlinear effects [22, 23]. Even recent machine learning models, while promising in prediction, are often based on limited datasets that restrict validation [24, 25].

Recent publications confirm these shortcomings. Studies on low-carbon cement pastes reported reduced flowability with ashes but used only single-factor analysis [26]. Other works showed that polymer admixtures significantly modify viscosity and yield stress but lacked multi-parameter optimization [27]. Investigations of structural build-up highlighted microstructural mechanisms but did not extend to predictive modelling [28]. In sustainable concretes with shea nutshell ash or groundnut shell ash, RSM and Box–Behnken optimization were applied, but the focus was largely on strength and durability [29, 30]. Richards et al. [31] demonstrated the rheological behavior of fresh cement suspensions, confirming the complexity of paste as a non-Brownian system. Studies in 2024 and 2025 further applied CCD and RSM to optimize recycled aggregate concretes, alkali-activated systems, and ternary blends, with positive results but limited emphasis on fresh-state rheology [32–36].

Building on this literature review, it becomes clear that important gaps remain in the current state of knowledge. First, although recent research has increasingly recognized the importance of rheology, most optimization studies still concentrate on hardened properties such as compressive strength, shrinkage, or durability, with comparatively little attention devoted to early-age behavior. Second, when fresh-state properties are considered, the majority of investigations fail to capture the inherently nonlinear nature of these systems. Interactions among key parameters such as w/c, w/p, and Sp/p are often simplified or examined in isolation, which limits the capacity to develop comprehensive predictive models. Third, many experimental programs continue to rely on single-factor or trial-and-error strategies. While straightforward, these approaches are inefficient, require large numbers of tests, and are incapable of representing the multi-parameter interactions that govern the performance of cementitious pastes.

The present study addresses these shortcomings by applying a Central Composite Design (CCD), a robust RSM variant, to systematically study the influence of three key parameters: water-to-cement ratio (w/c), water-to-powder ratio (w/p), and superplasticizer-to-powder ratio (Sp/p). Unlike most prior works focusing mainly on compressive strength, this research emphasizes fresh-state flow measured by mini-slump and Marsh funnel tests. CCD allows modelling of linear, quadratic, and interaction effects, generating predictive equations with fewer experiments [37–39].

The novelty of this work lies in combining CCD with practical rheological testing to build reliable predictive models. By identifying both primary and interaction effects, the methodology enables simulation and optimization of paste behavior, overcoming the limitations of conventional one-variable approaches.

This paper is Part II of a broader program. Part I applied a single-variable strategy, which provided insights into isolated effects but required many tests and did not capture nonlinearities. In contrast, Part II employs CCD to achieve deeper understanding with fewer experiments while enabling optimization. Together, these complementary approaches demonstrate the advantages of CCD for the systematic investigation of cement paste rheology [40–43].

2. Central Composite Design

2.1. Principles and Framework of RSM

Response Surface Methodology (RSM) is a powerful statistical tool used to model and analyze problems in which a response of interest is influenced by several input variables, with the objective of optimizing this response. In the context of materials science, RSM enables the prediction of material properties based on experimental factors—such as mix composition or processing conditions—and thus guides the formulation of optimal mixtures before physical testing. A factor in RSM refers to an independent variable that is deliberately controlled in the experimental setup, while the response refers to the measured outcome, such as flowability or viscosity.

One of the key strengths of RSM lies in its structured approach to experimentation. It employs carefully sequenced Design of Experiments (DOE) strategies to collect data efficiently and fit mathematical models, usually polynomial equations, to the observed responses. This approach allows for the identification not only of the main effects of individual variables but also of interaction effects and quadratic (nonlinear) relationships that are often present in complex systems such as cement-based materials [37–40]. RSM is particularly advantageous when the objective is to enhance the "signal" of a treatment effect or to explore multidimensional parameter spaces. By applying regression analysis and analysis of variance (ANOVA), it becomes possible to derive predictive models that simulate the influence of multiple factors simultaneously. These capabilities make RSM an ideal framework for optimization, sensitivity analysis, or process robustness assessment [41–43].

A significant advantage of RSM is its ability to reduce the number of experimental trials required to obtain statistically valid conclusions, without compromising reliability. This is especially beneficial in material development,

where each test may be time-consuming or resource-intensive. Moreover, RSM offers high flexibility by allowing researchers to consolidate several phases of experimentation into a single, coherent design, streamlining the research process [35, 44].

Several well-established RSM variants exist, most derived from factorial principles. These include: (i) full factorial designs, which explore all possible factor combinations; (ii) fractional factorial designs, which use a subset of combinations to reduce trials; (iii) Central Composite Designs (CCD), which extend factorial designs with axial (star) and center points to capture curvature; (iv) Box–Behnken designs, efficient for fitting second-order models with fewer runs than CCDs; (v) Koshal designs, designed to minimize the number of runs while maintaining model quality; (vi) Plackett–Burman designs, focused on screening large numbers of variables; and (vii) Taguchi orthogonal arrays, emphasizing robustness and variability control [42–45].

In this research, a CCD was selected as one of the most reliable RSM variants for fitting second-order models. CCD balances model accuracy and experimental efficiency, particularly in studies involving three or more variables, as it enables the modelling of curvature and the estimation of interactions. Figure 1 compares layouts of different RSM designs—full factorial, CCD, Box–Behnken, and Koshal—for three variables, illustrating CCD's advantage in capturing nonlinear behavior essential for predictive modelling.

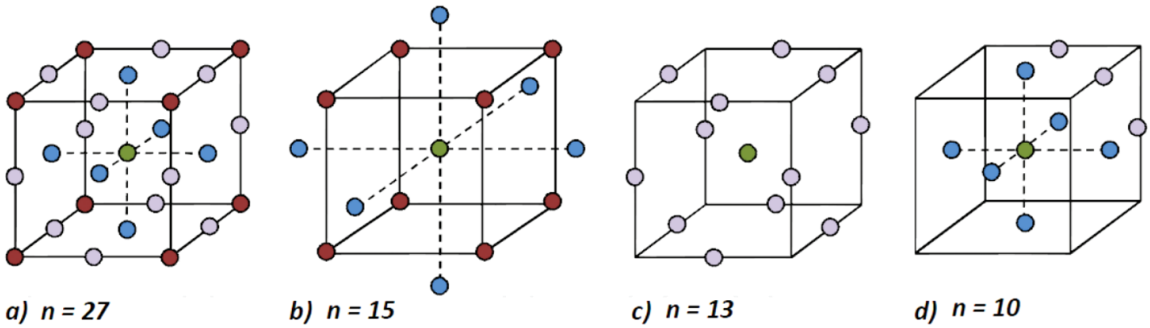

Figure 1. Experimental tests in three variables for: a) Full factorial design, b) central composite design, c) box-behnken design and d) Koshal design

2.2. CCD in Cementitious Materials and Methodology of the Present Study

The CCD is an adaptation of the factorial design, expanded with axial and center points. This structure allows for estimation of curvature and improves the modelling of first- and second-order terms. It also incorporates desirable statistical properties such as orthogonal blocks, which allow block effects to be estimated independently, minimizing variation in regression coefficients, and rotatability, which ensures constant prediction variance at points equidistant from the design center [17, 18]. Figure 2 shows a three-factor CCD with rotatability.

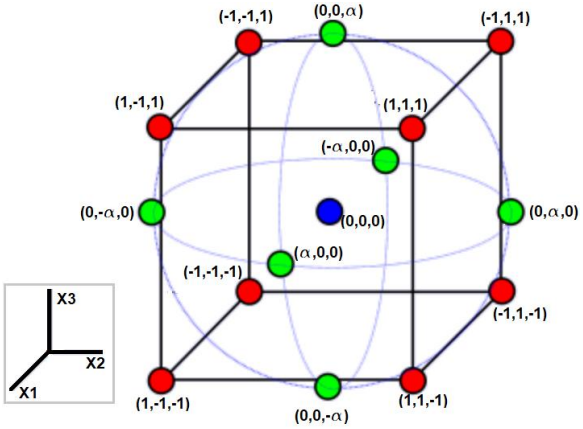

Figure 2. Three factor central composition design with rotatability

For a CCD with three factors, there are 15 trials defined by coded levels (−1, 0, +1, and axial). These are translated into real values for each factor, and the observations for each response can be fitted using a second-order polynomial:

$$Y = b_0 + b_1.X_1 + b_2.X_2 + b_3.X_3 + b_{12}.X_1.X_2 + b_{13}.X_1.X_3 + b_{23}.X_2.X_3 + b_{11}.X_1^2 + b_{22}.X_2^2 + b_{33}.X_3^2 \quad (1)$$

where X1, X_2 and X_3 are the factors (i.e. the independent variables); b_0 is the regression coefficient at the center point; b_1, b_2 and b_3 are linear coefficients; b_{12}, b_{13} and b_{23} are second order coefficients; and b_{11}, b_{22} and b_{33} are quadratic

coefficients. All the coefficients are obtained with statistics with the quality of the response (the fit of polynomial model equation) expressed by the coefficient of determination, R^2.

The experimental design and statistical analyses were performed using Design-Expert® software (Stat-Ease Inc., Minneapolis, MN, USA). Different software versions were used during the study. Figure 3 presents the methodological workflow, linking factor selection, mix preparation, testing, modelling, and optimization.

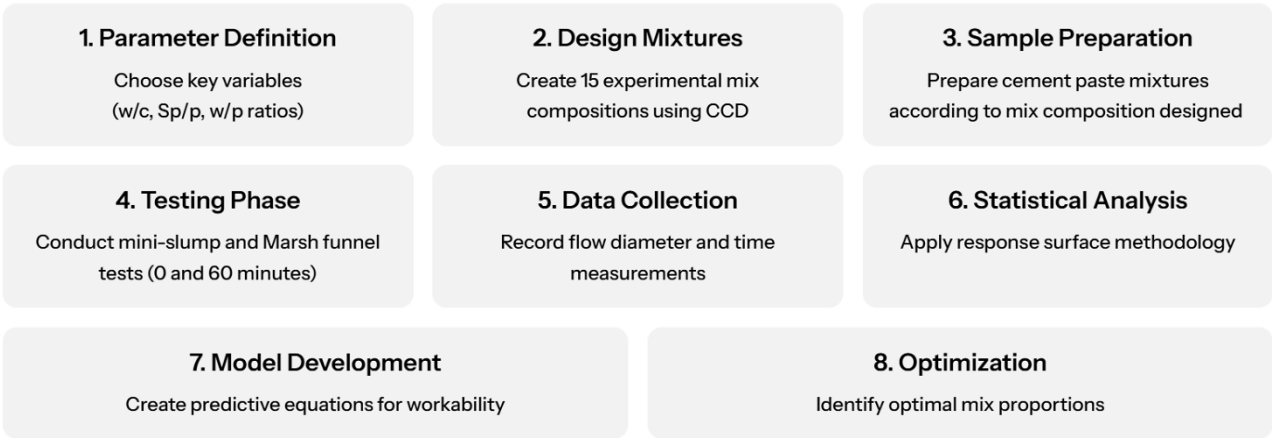

Figure 3. Flowchart of the methodology

2.3. Comparative Assessment and Relevance

Compared with other DOE strategies, CCD strikes an effective balance between statistical robustness and experimental feasibility. Full factorial designs quickly become impractical with more factors, while fractional factorials cannot detect curvature. Box–Behnken avoids extreme factor levels, which may be critical in rheological studies, and Taguchi methods emphasize robustness but lack direct quadratic modelling [43, 44]. CCD thus emerges as a rigorous and efficient option.

The theoretical strengths of CCD lie in its capacity to achieve rotatability and orthogonality. These properties ensure reliable predictions across the factor space and minimize confounding effects, which is particularly relevant when studying the combined effects of water-to-cement ratio, water-to-powder ratio, and superplasticizer-to-powder ratio in cementitious systems. Rheological parameters such as yield stress and viscosity arise from complex particle interactions and hydration kinetics, and CCD provides a statistical framework to model these phenomena as structured nonlinear effects.

Recent studies confirm CCD's effectiveness: Yu et al. [46] optimized UHPC with nano-silica; Rojo-López et al. [47] applied CCD to SCC blends; Sobuz et al. [48] integrated RSM with ML for SCC; Xu et al. [27] studied alkali-activated pastes; and Hayek et al. [21] modeled structural build-up. These examples reinforce CCD's suitability for advanced cementitious materials.

For the present work, CCD provides a principled approach to explore the combined influence of the three parameters under study. Unlike the one-variable-at-a-time method applied in Part I, CCD captures linear, quadratic, and interaction effects simultaneously, generating predictive models with reduced experimental effort. More importantly, CCD translates raw experimental scatter into meaningful insights into mechanisms governing fresh properties.

In summary, CCD was selected because it (i) comprehensively models linear, quadratic, and interaction effects, (ii) reduces experimental trials compared with factorial methods while preserving rigor, and (iii) has proven applicability in recent research. By embedding statistical robustness into experimental design, CCD bridges theoretical modelling with practical optimization, making it the most suitable DOE framework for this study.

3. Experimental Program

3.1. Materials and Mix Compositions

The 15 cement-based pastes were prepared using two powders: (i) commercial cement CEM I 42.5R (EN 197-1) containing 90.2% clinker, 5.2% gypsum, and 4.5% limestone filler, and (ii) limestone filler. Their specific gravities were 3.11 and 2.70 g/cm³, respectively. A third-generation superplasticizer with 40% solid content and a specific gravity of 1.08 g/cm³ was used. All mixtures were prepared with distilled water. The 15 mix compositions were arranged by varying the input parameters: water-to-cement ratio (w/c), superplasticizer-to-powder ratio (Sp/p), and water-to-powder ratio (w/p). All mixtures were prepared in a single batch with a total volume of 1.40 L.

The compositions of the 15 mixtures were defined based on a central composite design with three input variables (A, B, and C) corresponding to the parameters w/c, Sp/p, and w/p, respectively. The mix with coded values A = w/c = 0, B = Sp/p = 0, and C = w/p = 0 (i.e., the central composition) had actual values of w/c = 0.2886, Sp/p = 0.80%, and w/p = 0.5333. Relative to the central composition, the maximum variations of the input parameters were 6.3%, 25.0%, and 10.0% for w/c, Sp/p, and w/p, respectively. Regarding the constituent materials relative to the central composition, the maximum changes were: cement 6.7%, limestone filler 18.9%, superplasticizer 25.0%, and water 6.5%. No repetitions were performed, including for the central composition. Table 1 presents the data corresponding to each mixture of the central composite design.

Table 1. Mixtures of the central composite design

Mix order		Coded Values			Actual Values			Mass for batch [g]			
std	run	w/c	Sp/p	w/p	w/c	Sp/p	w/p	cem	Filler	Sp	water
1	14	-1	-1	-1	0.2796	0.0070	0.5066	1690.3	1046.7	19.159	461.15
2	15	1	-1	-1	0.2977	0.0070	0.5066	1587.9	1136.0	19.067	461.21
3	13	-1	1	-1	0.2796	0.0090	0.5066	1690.3	1046.7	24.634	457.87
4	12	1	1	-1	0.2977	0.0090	0.5066	1587.9	1136.0	24.515	457.94
5	10	-1	-1	1	0.2796	0.0070	0.5600	1804.4	861.3	18.660	493.35
6	11	1	-1	1	0.2977	0.0070	0.5600	1695.0	956.5	18.561	493.41
7	9	-1	1	1	0.2796	0.0090	0.5600	1804.4	861.3	23.991	490.15
8	8	1	1	1	0.2977	0.0090	0.5600	1695.0	956.5	23.864	490.23
9	2	-1.6818	0	0	0.2706	0.0080	0.5333	1806.6	901.6	21.666	475.88
10	3	1.6818	0	0	0.3067	0.0080	0.5333	1594.1	1086.8	21.447	476.01
11	4	0	-1.6818	0	0.2886	0.0060	0.5333	1693.7	1000.0	16.162	479.18
12	5	0	1.6818	0	0.2886	0.0100	0.5333	1693.7	1000.0	26.937	472.71
13	7	0	0	-1.6818	0.2886	0.0080	0.4800	1579.3	1188.9	22.145	442.55
14	6	0	0	1.6818	0.2886	0.0080	0.5866	1800.5	823.8	20.994	507.09
15	1	0	0	0	0.2886	0.0080	0.5333	1693.7	1000.0	21.550	475.95

3.2. Mixing and Testing

Batches were prepared using a mixer typically employed for standard paste tests according to European Norm 196 [49]. However, the mixing procedure was adjusted as follows: (i) the cement, limestone filler, superplasticizer, and water were weighed separately in plastic containers; (ii) cement and limestone filler were placed in the mixing container, and approximately 80% of the water was added; (iii) mixing was performed for 60 seconds at low speed; (iv) mixing was stopped while the remaining water and superplasticizer were added on top of the paste; (v) mixing resumed for 60 seconds at low speed; (vi) mixing was stopped for 30 seconds; (vii) mixing continued for 120 seconds at low speed; (viii) mixing was stopped for 15 seconds; and (ix) mixing finished with 30 seconds at high speed.

Immediately after mixing, workability was assessed using the flow and Marsh funnel tests. The flow test was conducted twice, while the Marsh funnel test was performed once. For each individual flow test, the flow diameter was measured in two orthogonal directions. Therefore, in this paper, the flow test result is the average of four readings (D0'1a, D0'1b, D0'2a, D0'2b), whereas the Marsh funnel test result corresponds to a single reading (t0). These workability tests were repeated 60 minutes after the start of mixing, with the readings D60'1a, D60'1b, D60'2a, D60'2b, and t60 taken at that time.

As described in Part I, a downscaled Abrams cone geometry was used for the mini-slump test [7, 8], with dimensions of 57 mm height, 19 mm top diameter, and 38 mm bottom diameter. The Marsh funnel (EN 445 [50]) was adapted for cement-based pastes by pouring 1000 ml of paste into the setup and measuring the flow time for 500 ml.

3.3. Experimental Results Recorded

Table 2 presents the recorded and calculated results of the flow test and the Marsh funnel test. Note that the D0 value is the average of the readings D0'1a, D0'1b, D0'2a, and D0'2b, while the D60 value is the average of the readings D60'1a, D60'1b, D60'2a, and D60'2b. The t0 and t60 values are obtained directly from the readings.

Table 2. Results from the flow test [cm] and the Marsh funnel test [s]

Mix order		Immediately after mixing						60 minutes after mixing					
std	**run**	**D0'1a**	**D0'1b**	**D0'2a**	**D0'2b**	**D0**	**t0**	**D60'1a**	**D60'1b**	**D60'2a**	**D60'2b**	**D60**	**t60**
1	14	19.8	19.6	20.0	20.4	**19.95**	**82.50**	19.2	19.3	19.1	19.1	**19.18**	**140.12**
2	15	20.1	20.0	20.5	20.5	**20.28**	**80.06**	18.9	19.0	19.5	19.3	**19.18**	**138.69**
3	13	20.2	20.1	20.2	20.5	**20.25**	**78.50**	18.8	18.9	19.9	19.8	**19.35**	**107.75**
4	12	19.6	19.7	20.2	20.2	**19.93**	**76.09**	20.0	20.0	19.0	18.8	**19.45**	**100.03**
5	10	17.5	18.0	18.5	18.5	**18.13**	**67.50**	18.6	18.6	18.5	18.0	**18.43**	**112.72**
6	11	20.1	20.2	19.3	18.9	**19.63**	**63.03**	19.9	19.8	19.0	20.0	**19.68**	**90.44**
7	9	21.5	21.0	21.4	21.5	**21.35**	**61.56**	21.5	21.0	21.0	21.5	**21.25**	**87.28**
8	8	21.9	21.9	22.3	21.5	**21.90**	**59.34**	20.3	20.9	21.0	20.9	**20.78**	**75.78**
9	2	20.5	20.5	19.1	19.8	**19.98**	**68.46**	20.3	20.3	20.2	20.0	**20.20**	**109.87**
10	3	21.6	21.6	20.5	21.0	**21.18**	**57.82**	20.6	20.5	20.3	20.3	**20.43**	**85.78**
11	4	19.6	19.6	19.5	19.4	**19.53**	**78.34**	17.0	17.2	16.6	16.6	**16.85**	**215.80**
12	5	21.1	21.1	19.3	19.9	**20.35**	**67.37**	20.6	20.7	19.3	19.1	**19.93**	**86.56**
13	7	18.1	18.6	19.3	19.2	**18.80**	**87.97**	18.3	18.5	18.5	18.4	**18.43**	**144.03**
14	6	22.0	21.8	22.4	21.5	**21.93**	**53.03**	22.0	22.0	22.0	21.5	**21.88**	**74.34**
15	1	20.6	20.4	20.1	20.1	**20.30**	**70.97**	19.8	20.1	20.1	20.0	**20.00**	**105.25**
Minimum						18.13	53.03					16.85	74.34
Maximum						21.93	87.97					21.88	215.80
Average						20.23	70.17					19.67	111.62
Std. Deviation						1.01	9.82					1.19	35.26
Coef. Variation						5.0%	14.0%					6.1%	31.6%

4. Analyses of Results, Response Models and Discussion

4.1. Previous Analysis of the Results Recorded

Analysis of the results was supported by the Design-Expert® software (Stat-Ease, Inc.) and its User's Guide [51]. Since the DOE was developed based on a central composite design, the software offers several options. Among these, it allows the inclusion of constituent materials as response variables. Although the constituent materials are entirely calculated based on the input variables, introducing their values enables additional analyses, such as examining correlations with other variables.

Before proceeding to response modeling, quick observations were made from the overall results presented in Table 2. The flow time in the Marsh funnel showed greater variation than the flow diameter, both immediately after mixing and 60 minutes later. In fact, the output values for D0 and D60 are noticeably closer to the average compared to t0 and t60. Furthermore, greater changes were observed between t0 and t60 than between D0 and D60, indicating that the flow time in the Marsh funnel is more affected by the test duration than the flow diameter.

Prior to applying response models, the software allows a preliminary analysis of all variables (both input and response) to detect correlations. These correlations can be presented in a correlation matrix (Figure 4) or graphically for specific variable pairs (Figures 5 and 6). Analyzing Figure 4 reveals that the strongest correlation is between w/p and t0, indicating that this response variable is mainly influenced by w/p. For D0, t60, and D60, Sp/p shows the highest correlations, although significant correlations with w/p are also observed. The w/c is the input variable with the lowest correlation to the workability variables. Indeed, when comparing with material contents, Figure 4 shows that the correlation between cement content and workability variables is generally stronger than that of w/c. Correlations are also found among response variables; for example, t60 has a high correlation with all other workability variables (t0, D0, and D60). Conversely, low correlations exist between some variables, such as between w/c and D60 (Figure 5) and between Sp/p and t0 (Figure 6).

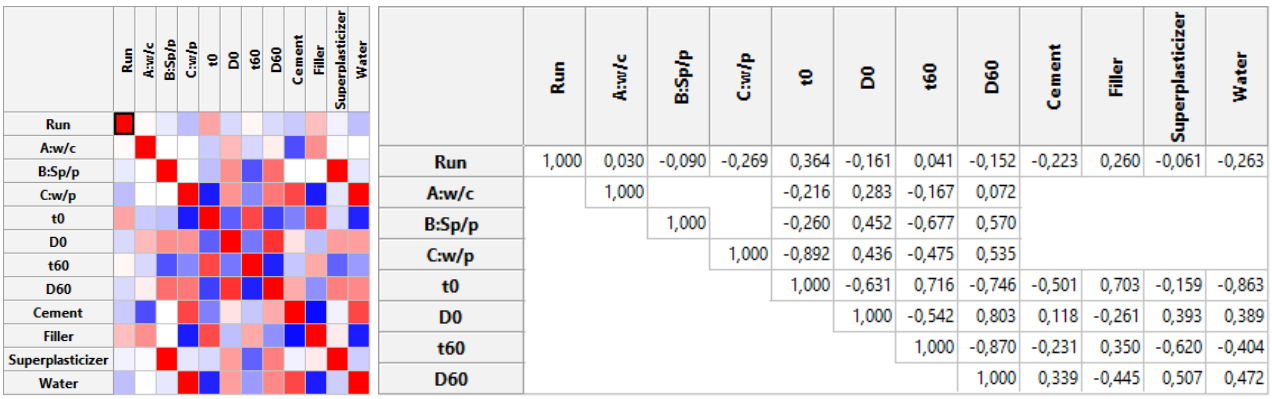

	Run	A:w/c	B:Sp/p	C:w/p	t0	D0	t60	D60	Cement	Filler	Superplasticizer	Water
Run	1,000	0,030	-0,090	-0,269	0,364	-0,161	0,041	-0,152	-0,223	0,260	-0,061	-0,263
A:w/c		1,000			-0,216	0,283	-0,167	0,072				
B:Sp/p			1,000		-0,260	0,452	-0,677	0,570				
C:w/p				1,000	-0,892	0,436	-0,475	0,535				
t0					1,000	-0,631	0,716	-0,746	-0,501	0,703	-0,159	-0,863
D0						1,000	-0,542	0,803	0,118	-0,261	0,393	0,389
t60							1,000	-0,870	-0,231	0,350	-0,620	-0,404
D60								1,000	0,339	-0,445	0,507	0,472

Figure 4. Correlation matrix of the variables

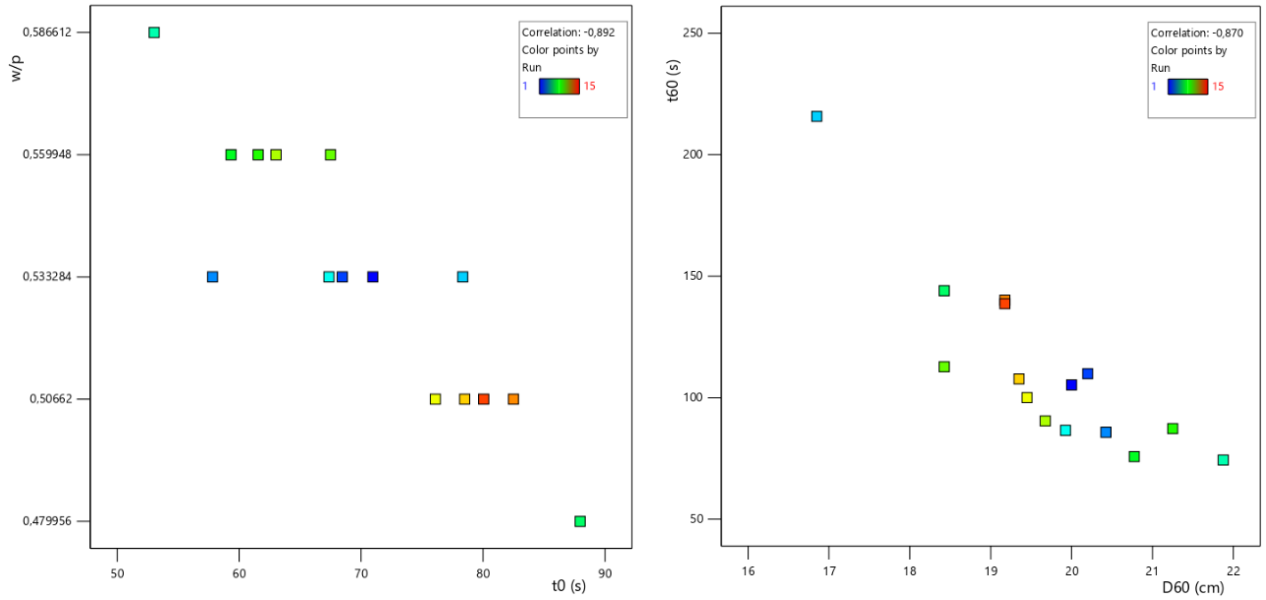

Figure 5. Graphical examples of detected correlations: (a) between the input parameter w/p versus the response variable t0, (b) between the response variables t60 versus D60

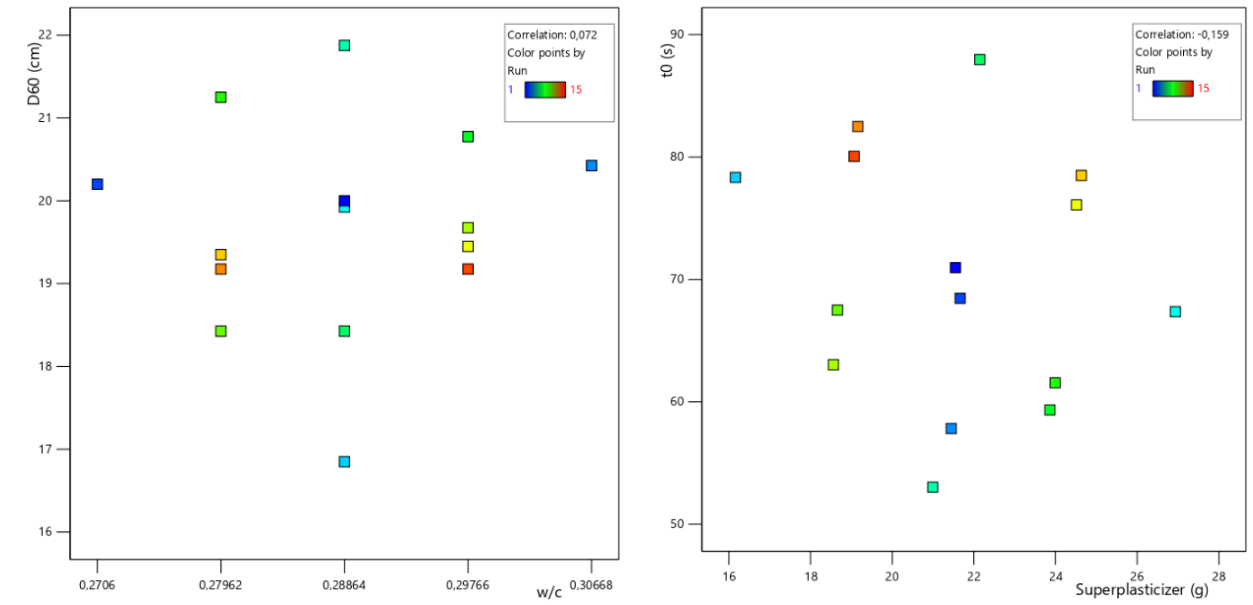

Figure 6. Graphical examples of undetected correlations: (a) between the response variable D60 versus the input parameter w/c, (b) between the response variable t0 versus the superplasticizer content

4.2. Application and Analyses of Response Models

As previously explained, the great advantage of running the DOE according to a central composite design, is the possibility to apply response models. Here, in this sub-section response models are applied and its applicability is discussed.

4.2.1. Response Variable t0

When evaluating the response variable t0, which corresponds to the initial flow time immediately after mixing, the statistical software first suggested a quadratic model as the most suitable representation of the experimental data (Figure 7). This recommendation was based on multiple statistical criteria. Among the tested alternatives, the quadratic model was the only one that fulfilled the requirement of significance, as evidenced by a p-value below 0.05. In addition, it presented the highest Adjusted R^2 and Predicted R^2 values, indicating both explanatory power and good predictive ability. These indicators provided confidence that the quadratic model would adequately capture the complexity of the system.

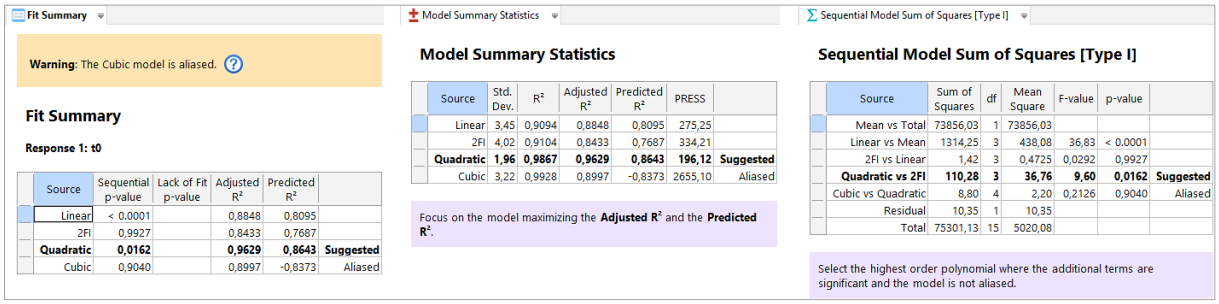

Fit Summary

Warning: The Cubic model is aliased.

Fit Summary

Response 1: t0

Source	Sequential p-value	Lack of Fit p-value	Adjusted R^2	Predicted R^2	
Linear	< 0.0001		0,8848	0,8095	
2FI	0,9927		0,8433	0,7687	
Quadratic	**0,0162**		**0,9629**	**0,8643**	**Suggested**
Cubic	0,9040		0,8997	-0,8373	Aliased

Model Summary Statistics

Model Summary Statistics

Source	Std. Dev.	R^2	Adjusted R^2	Predicted R^2	PRESS	
Linear	3,45	0,9094	0,8848	0,8095	275,25	
2FI	4,02	0,9104	0,8433	0,7687	334,21	
Quadratic	**1,96**	**0,9867**	**0,9629**	**0,8643**	**196,12**	**Suggested**
Cubic	3,22	0,9928	0,8997	-0,8373	2655,10	Aliased

Focus on the model maximizing the **Adjusted R^2** and the **Predicted R^2**.

Sequential Model Sum of Squares [Type I]

Sequential Model Sum of Squares [Type I]

Source	Sum of Squares	df	Mean Square	F-value	p-value	
Mean vs Total	73856,03	1	73856,03			
Linear vs Mean	1314,25	3	438,08	36,83	< 0.0001	
2FI vs Linear	1,42	3	0,4725	0,0292	0,9927	
Quadratic vs 2FI	**110,28**	**3**	**36,76**	**9,60**	**0,0162**	**Suggested**
Cubic vs Quadratic	8,80	4	2,20	0,2126	0,9040	Aliased
Residual	10,35	1	10,35			
Total	75301,13	15	5020,08			

Select the highest order polynomial where the additional terms are significant and the model is not aliased.

Figure 7. Preliminary information given by the software for modelling the t0

Once the quadratic model was selected, an Analysis of Variance (ANOVA) was performed (Figure 8). The ANOVA output confirmed the global significance of the model and allowed the partitioning of variance among individual terms. The most striking result was that the water-to-powder ratio (w/p) emerged as the dominant factor influencing t0. Its contribution was considerably higher than the other two variables, accounting for the majority of the variability in the response. Nevertheless, the water-to-cement ratio (w/c) and the superplasticizer-to-powder ratio (Sp/p) also exhibited statistically significant effects. Their influence was estimated to be approximately one quarter of the effect of w/p, highlighting that although secondary, these parameters cannot be disregarded. Moreover, the quadratic term $(w/p)^2$ was statistically relevant, reinforcing the nonlinear nature of the relationship. The magnitude of its contribution was comparable to that of w/c and Sp/p, further justifying the adoption of a second-order model.

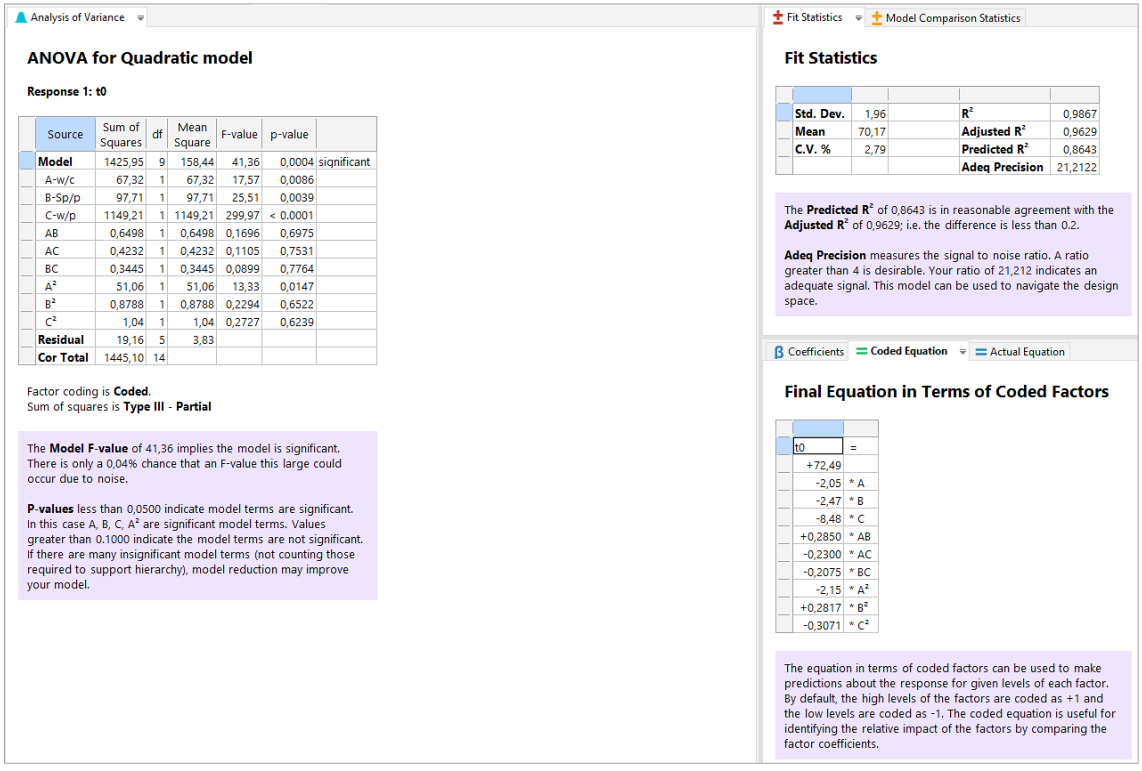

Analysis of Variance

ANOVA for Quadratic model

Response 1: t0

Source	Sum of Squares	df	Mean Square	F-value	p-value	
Model	1425,95	9	158,44	41,36	0,0004	significant
A-w/c	67,32	1	67,32	17,57	0,0086	
B-Sp/p	97,71	1	97,71	25,51	0,0039	
C-w/p	1149,21	1	1149,21	299,97	< 0.0001	
AB	0,6498	1	0,6498	0,1696	0,6975	
AC	0,4232	1	0,4232	0,1105	0,7531	
BC	0,3445	1	0,3445	0,0899	0,7764	
A^2	51,06	1	51,06	13,33	0,0147	
B^2	0,8788	1	0,8788	0,2294	0,6522	
C^2	1,04	1	1,04	0,2727	0,6239	
Residual	19,16	5	3,83			
Cor Total	1445,10	14				

Factor coding is **Coded**.
Sum of squares is **Type III - Partial**

The **Model F-value** of 41,36 implies the model is significant. There is only a 0,04% chance that an F-value this large could occur due to noise.

P-values less than 0,0500 indicate model terms are significant. In this case A, B, C, A^2 are significant model terms. Values greater than 0.1000 indicate the model terms are not significant. If there are many insignificant model terms (not counting those required to support hierarchy), model reduction may improve your model.

Fit Statistics | Model Comparison Statistics

Fit Statistics

Std. Dev.	1,96	**R^2**	0,9867
Mean	70,17	**Adjusted R^2**	0,9629
C.V. %	2,79	**Predicted R^2**	0,8643
		Adeq Precision	21,2122

The **Predicted R^2** of 0,8643 is in reasonable agreement with the **Adjusted R^2** of 0,9629; i.e. the difference is less than 0.2.

Adeq Precision measures the signal to noise ratio. A ratio greater than 4 is desirable. Your ratio of 21,212 indicates an adequate signal. This model can be used to navigate the design space.

Coefficients | Coded Equation | Actual Equation

Final Equation in Terms of Coded Factors

t0	=
+72,49	
-2,05	* A
-2,47	* B
-8,48	* C
+0,2850	* AB
-0,2300	* AC
-0,2075	* BC
-2,15	* A^2
+0,2817	* B^2
-0,3071	* C^2

The equation in terms of coded factors can be used to make predictions about the response for given levels of each factor. By default, the high levels of the factors are coded as +1 and the low levels are coded as -1. The coded equation is useful for identifying the relative impact of the factors by comparing the factor coefficients.

Figure 8. Analysis of variance and statistics data and comments for the quadratic model applied to the t0

The adequacy of the model was subsequently verified through residual diagnostics. Figures 9-a to 9-d provides a comprehensive set of statistical checks. The normal probability plot of residuals showed that the residuals closely followed the straight reference line, confirming that the assumption of normality was satisfied. The predicted versus actual values aligned along the 45° line, indicating strong agreement between experimental and predicted values. The distribution of externally studentized residuals against predicted values demonstrated a random pattern around zero with no visible systematic trends. Finally, Cook's Distance revealed that all data points fell within acceptable thresholds, suggesting that no single observation exerted undue influence on the regression. Taken together, these analyses demonstrated that the quadratic model satisfied the key assumptions of regression analysis.

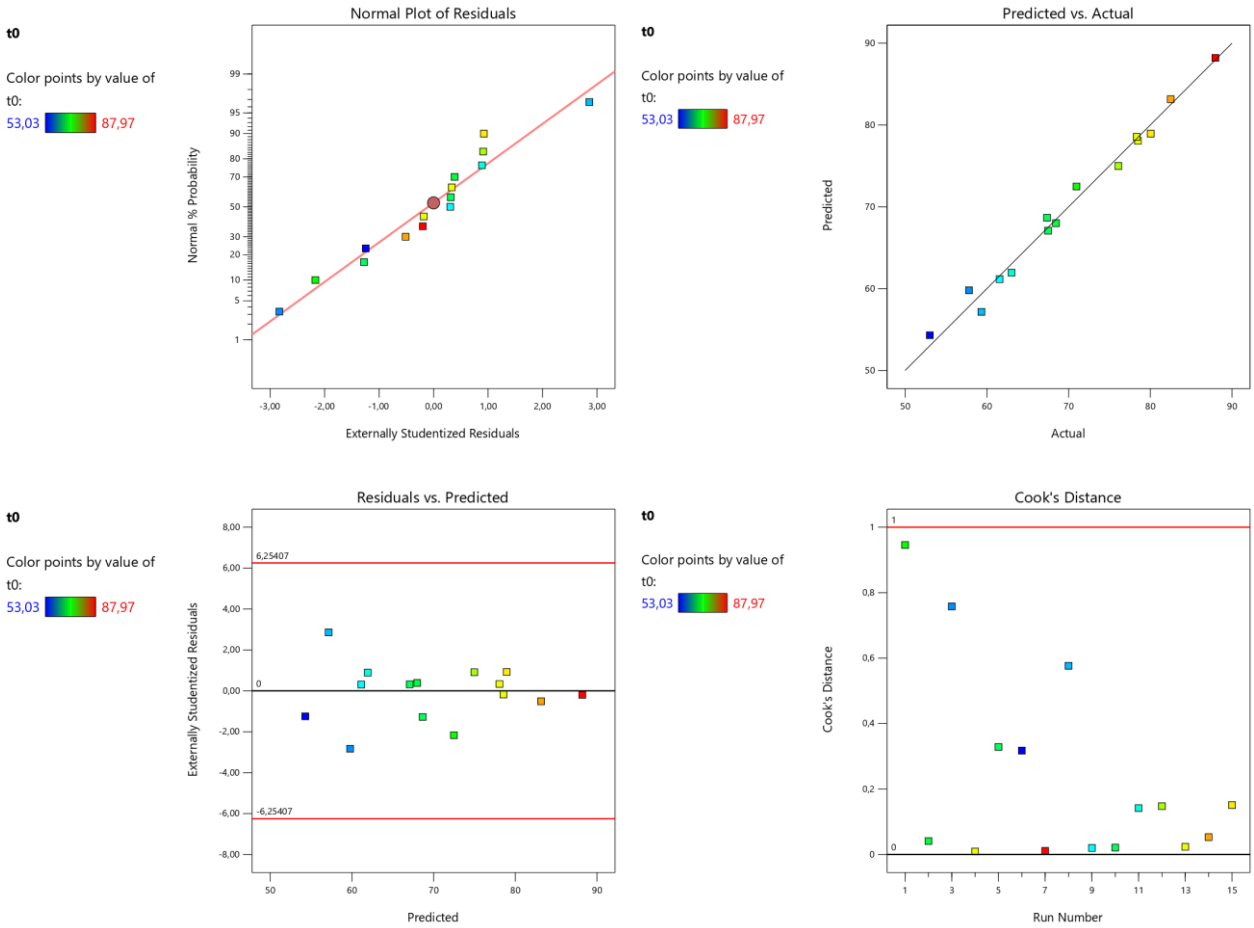

Figure 9. Analysis of the quadratic model applied to the t0: a) normal plot of residuals, b) plotted results of Predicted vs. Actual values, c) the Externally Studentized Residuals distribution vs. predicted, and d) the Cook's Distance

The fitted response surfaces are illustrated in Figure 10. The main effects plot (Figure 10-a) shows the predominant role of w/p, which strongly affects t0. In practical terms, increasing w/p reduces t0, accelerating the initial flow, although beyond certain limits it may compromise stability. The three-dimensional surface plot (Figure 10b) provides an intuitive visualization of how the combined variation of w/c and Sp/p modifies the response, while the cubic representation (Figure 10c) emphasizes the curvature introduced by the quadratic term $(w/p)^2$. The interaction plot (Figure 10d) further illustrates that cross-effects between the studied variables are minor compared to the main effects, as already indicated by the ANOVA results, since the interaction terms were not statistically significant ($p > 0.05$).

Overall, the analysis of t0 demonstrates that a quadratic model is not only statistically appropriate but also practically informative. It captures the overwhelming effect of w/p, while also accounting for the relevant but secondary influences of w/c and Sp/p. Furthermore, the inclusion of the quadratic term provides additional accuracy by reproducing the nonlinear trends inherent to cement-based systems. This level of detail is crucial for predictive modeling, as it allows researchers and practitioners to anticipate the consequences of modifying mix proportions. By integrating both statistical rigor and engineering interpretation, the model for t0 establishes a basis for optimization and for guiding the formulation of pastes with tailored fresh-state performance.

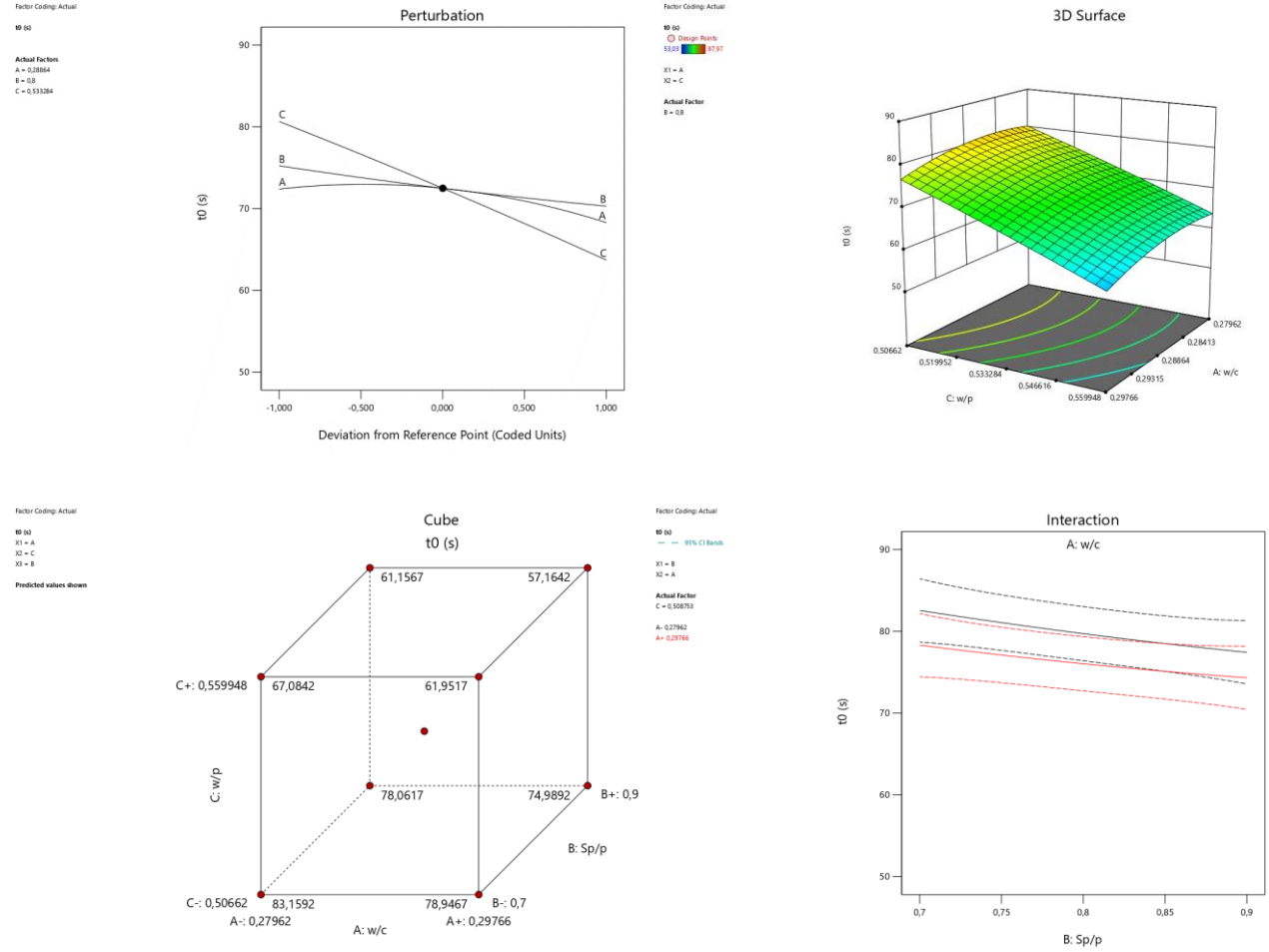

Figure 10. Plotted results of the t0: a) Primary effect of the input parameters, b) 3D model visualization, c) Cubic visualization of predicted values, and d) Interaction effect of the w/c and S/p

4.2.2. Response Variable D0

A similar procedure was applied to the response variable D0. However, for D0, as it is observed in Figure 11 the software suggested a two-factor interaction model. And, with the information of Figure 12 from the ANOVA, one concludes that the two-factor interaction model has a p-value lower that 0.05 (a necessary condition for a significant model). The Adeq Precision is acceptable; however, the Adjusted R^2 and Predicted R^2 values are not close. That means, although the software adjusts and provides a model, one shall keep in mind that the provided model may have low precision.

Fit Summary | Model Summary Statistics | Sequential Model Sum of Squares [Type I]

Warning: The Cubic model is aliased.

Fit Summary

Response 2: D0

Source	Sequential p-value	Lack of Fit p-value	Adjusted R^2	Predicted R^2	
Linear	0,0606		0,3321	0,0144	
2FI	**0,0619**		**0,6149**	**0,0336**	**Suggested**
Quadratic	0,8667		0,4608	-0,7483	
Cubic	0,1939		0,9544	0,1652	Aliased

Model Summary Statistics

Source	Std. Dev.	R^2	Adjusted R^2	Predicted R^2	PRESS	
Linear	0,8574	0,4752	0,3321	0,0144	15,18	
2FI	**0,6510**	**0,7800**	**0,6149**	**0,0336**	**14,89**	**Suggested**
Quadratic	0,7703	0,8074	0,4608	-0,7483	26,93	
Cubic	0,2239	0,9967	0,9544	0,1652	12,86	Aliased

Focus on the model maximizing the **Adjusted R^2** and the **Predicted R^2**.

Sequential Model Sum of Squares [Type I]

Source	Sum of Squares	df	Mean Square	F-value	p-value	
Mean vs Total	6138,79	1	6138,79			
Linear vs Mean	7,32	3	2,44	3,32	0,0606	
2FI vs Linear	**4,70**	**3**	**1,57**	**3,69**	**0,0619**	**Suggested**
Quadratic vs 2FI	0,4232	3	0,1411	0,2378	0,8667	
Cubic vs Quadratic	2,92	4	0,7291	14,54	0,1939	Aliased
Residual	0,0501	1	0,0501			
Total	6154,20	15	410,28			

Select the highest order polynomial where the additional terms are significant and the model is not aliased.

Figure 11. Preliminary information given by the software for modelling the D0

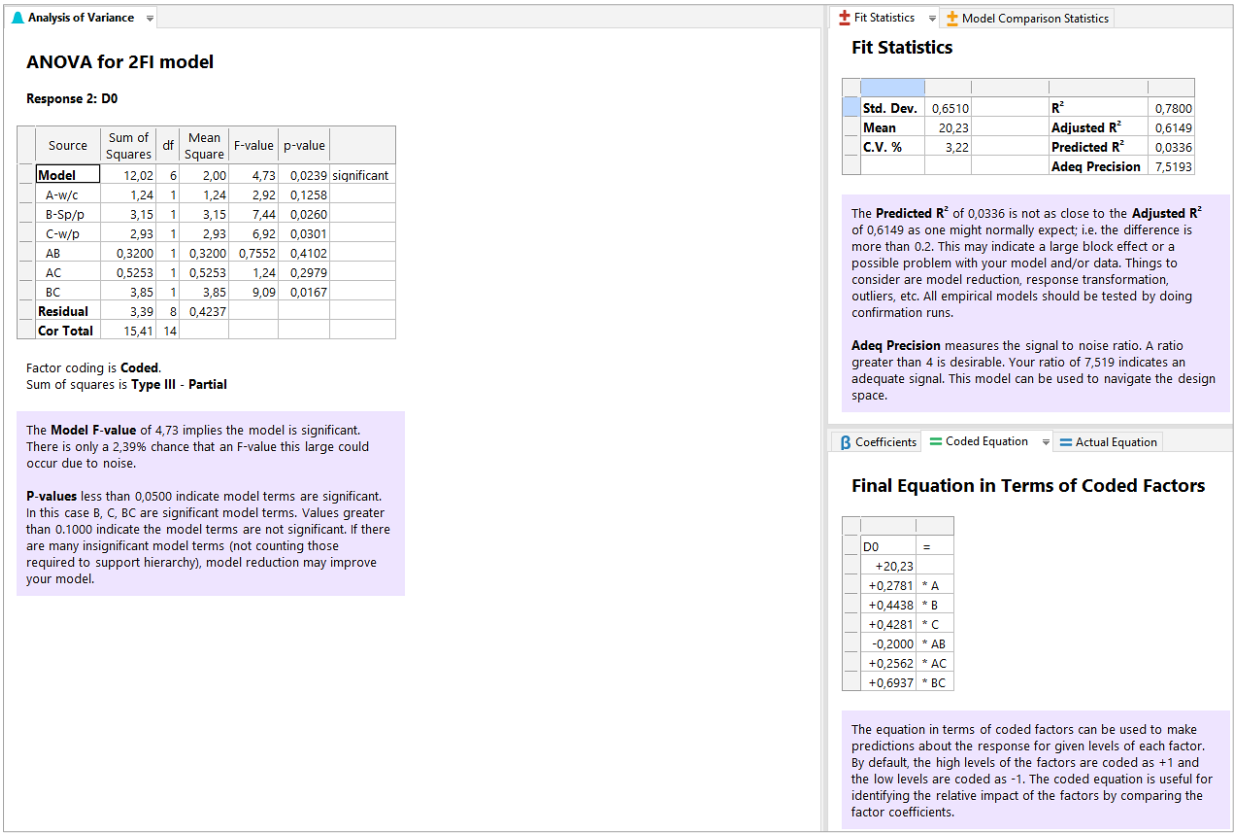

Analysis of Variance

ANOVA for 2FI model

Response 2: D0

Source	Sum of Squares	df	Mean Square	F-value	p-value	
Model	12,02	6	2,00	4,73	0,0239	significant
A-w/c	1,24	1	1,24	2,92	0,1258	
B-Sp/p	3,15	1	3,15	7,44	0,0260	
C-w/p	2,93	1	2,93	6,92	0,0301	
AB	0,3200	1	0,3200	0,7552	0,4102	
AC	0,5253	1	0,5253	1,24	0,2979	
BC	3,85	1	3,85	9,09	0,0167	
Residual	3,39	8	0,4237			
Cor Total	15,41	14				

Factor coding is **Coded**.
Sum of squares is **Type III - Partial**

The **Model F-value** of 4,73 implies the model is significant. There is only a 2,39% chance that an F-value this large could occur due to noise.

P-values less than 0,0500 indicate model terms are significant. In this case B, C, BC are significant model terms. Values greater than 0.1000 indicate the model terms are not significant. If there are many insignificant model terms (not counting those required to support hierarchy), model reduction may improve your model.

Fit Statistics | Model Comparison Statistics

Fit Statistics

Std. Dev.	0,6510	R^2	0,7800
Mean	20,23	**Adjusted R^2**	0,6149
C.V. %	3,22	**Predicted R^2**	0,0336
		Adeq Precision	7,5193

The **Predicted R^2** of 0,0336 is not as close to the **Adjusted R^2** of 0,6149 as one might normally expect; i.e. the difference is more than 0.2. This may indicate a large block effect or a possible problem with your model and/or data. Things to consider are model reduction, response transformation, outliers, etc. All empirical models should be tested by doing confirmation runs.

Adeq Precision measures the signal to noise ratio. A ratio greater than 4 is desirable. Your ratio of 7,519 indicates an adequate signal. This model can be used to navigate the design space.

Coefficients | Coded Equation | Actual Equation

Final Equation in Terms of Coded Factors

D0	=
+20,23	
+0,2781	* A
+0,4438	* B
+0,4281	* C
-0,2000	* AB
+0,2562	* AC
+0,6937	* BC

The equation in terms of coded factors can be used to make predictions about the response for given levels of each factor. By default, the high levels of the factors are coded as +1 and the low levels are coded as -1. The coded equation is useful for identifying the relative impact of the factors by comparing the factor coefficients.

Figure 12. Analysis of variance and statistics data and comments for the linear model with interaction effects applied to D0

According to the model, it is observed that the w/c ratio has a low impact on D0, with the Sp/p, the w/p and the interaction effect of these two variables controlling the response.

4.2.3. Response Variable t60

For the response variable t60, some adjustments to the response model were required. First, it was recommended apply a transform variable $t60^T = 1/\sqrt{t60}$ (see Figure 13). Second, then when the results were analyzed it was suggested that the value obtained for the mix order run#4 = 215.80 s should be an outlier, therefore should be excluded from the model. Therefore, an ANOVA with the new transformed variable was done without the value of the mix run#4 (the value was excluded from the analysis – the software placed a note in the ANOVA report – see Figure 14).

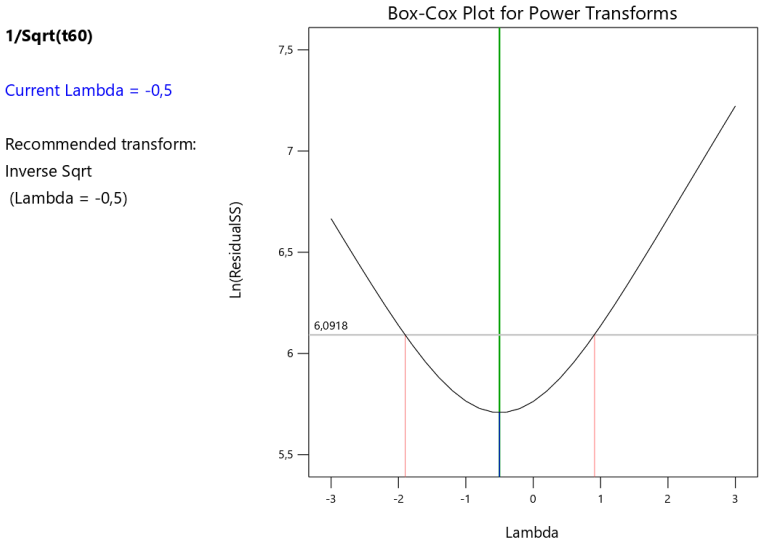

Figure 13. Transform variable is recommended for the t60

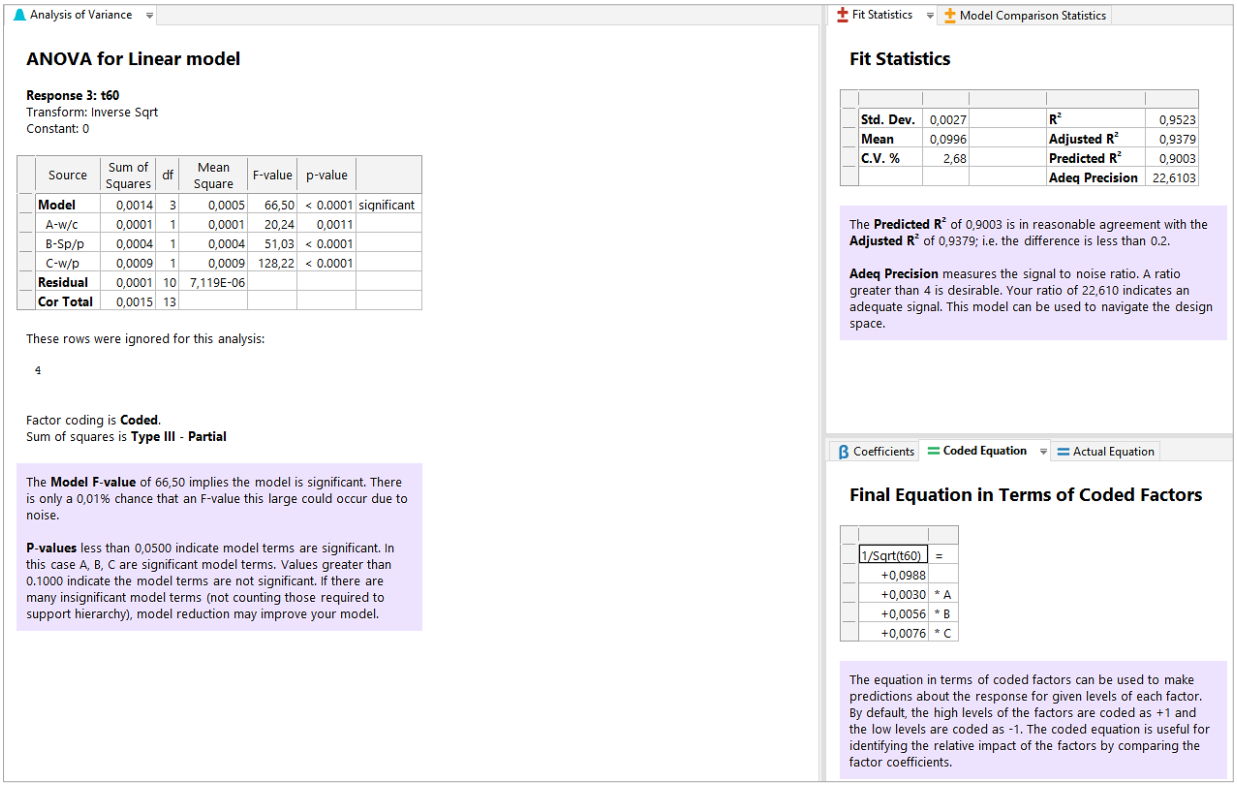

Figure 14. Analysis of variance and statistics data and comments for the linear model applied to the t60 with the transform variable being the Inverse Sqrt

With these two differences, a linear model for the response variable *t60* was determined. From the model and the ANOVA analyses, it can be observed that the linear model is significant and that all input parameters are significant, with the w/p ratio showing the greatest influence. Furthermore, the model demonstrates a good fit, as the Adeq Precision is markedly higher than 4, and the R^2, Adjusted R^2, and Predicted R^2 values are not only close to each other but also high. The software automatically provides graphs to assist in analyzing the ANOVA results. However, this information can also be presented in tabular form. Table 3 reports this information (note that run #4 is missing because it was excluded).

Table 3. Report of the ANOVA for the t60

Run Order	Actual Value	Predicted Value	Residual	Leverage	Internally Studentized Residuals	Externally Studentized Residuals	Cook's Distance	Influence on Fitted Value DFFITS	Standard Order
1	0.0975	0.0988	-0.0013	0.073	-0.524	-0.504	0.005	-0.142	15
2	0.0954	0.0928	0.0026	0.323	1.178	1.204	0.166	0.832	9
3	0.1080	0.1048	0.0031	0.323	1.435	1.527	0.246	1.055	10
5	0.1075	0.1100	-0.0025	0.366	-1.164	-1.188	0.196	-0.902	12
6	0.1160	0.1139	0.0021	0.323	0.936	0.930	0.105	0.643	14
7	0.0833	0.0837	-0.0004	0.323	-0.177	-0.168	0.004	-0.116	13
8	0.1149	0.1149	-0.0001	0.259	-0.030	-0.028	0.000	-0.017	8
9	0.1070	0.1089	-0.0019	0.259	-0.828	-0.814	0.060	-0.481	7
10	0.0942	0.0978	-0.0036	0.308	-1.628	-1.801	0.295	-1.202	5
11	0.1052	0.1038	0.0013	0.308	0.607	0.587	0.041	0.392	6
12	0.1000	0.0998	0.0001	0.259	0.065	0.062	0.000	0.036	4
13	0.0963	0.0938	0.0025	0.259	1.090	1.101	0.104	0.651	3
14	0.0845	0.0827	0.0018	0.308	0.804	0.788	0.072	0.526	1
15	0.0849	0.0887	-0.0038	0.308	-1.705	-1.920	0.323	-1.281	2

In Figure 15 one can observe the primary effects of each input parameter in t60. As previously mentioned, no interaction effects are detected in the model. Although being a linear model, the effects are mostly in agreement with the main effects of t0, with the w/p parameter playing the main role.

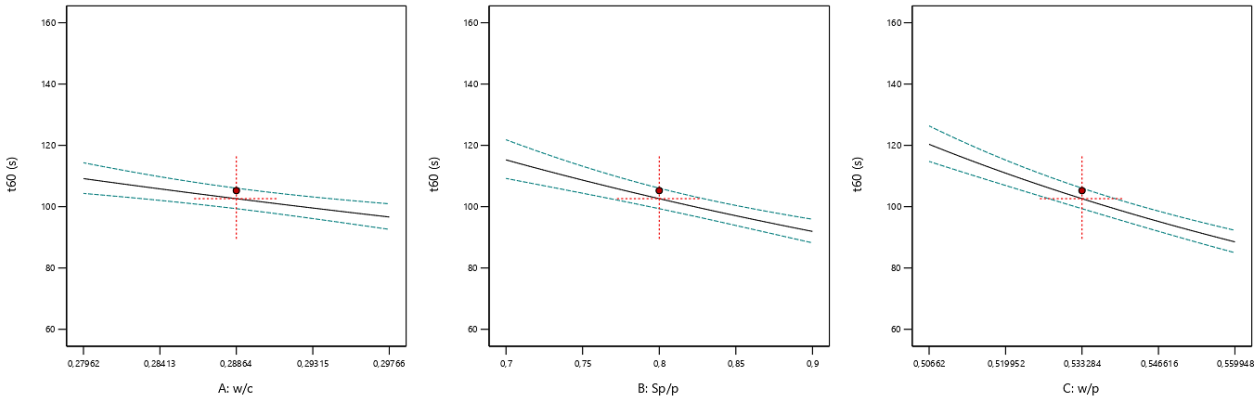

Figure 15. Primary effect of the input parameters for t60

4.3. Response Variable D60

Finally, the response variable *D60* was modeled. The initial analysis suggested a Quadratic Model; however, it was observed that the Adjusted R^2 and the Predicted R^2 were neither high nor close to each other (see Figure 16). Therefore, a model reduction to a linear model was selected to identify the main effects. The linear model was found to be significant, with a p-value of 0.0119 (which is lower than 0.05), and the Sp/p and w/p parameters were significant terms in the model (see Figure 17). Nevertheless, an analysis of Figure 17 shows that the Adjusted R^2 and Predicted R^2 values remain not only low but also not close to each other. This may be due to a block effect with high dispersion, as no outliers were identified. Overall, the model indicates that the coefficients of the significant parameters have similar weights, which is consistent with the findings for the response variable *D0* (although for *D0*, a strong interaction effect between Sp/p and w/p was also observed).

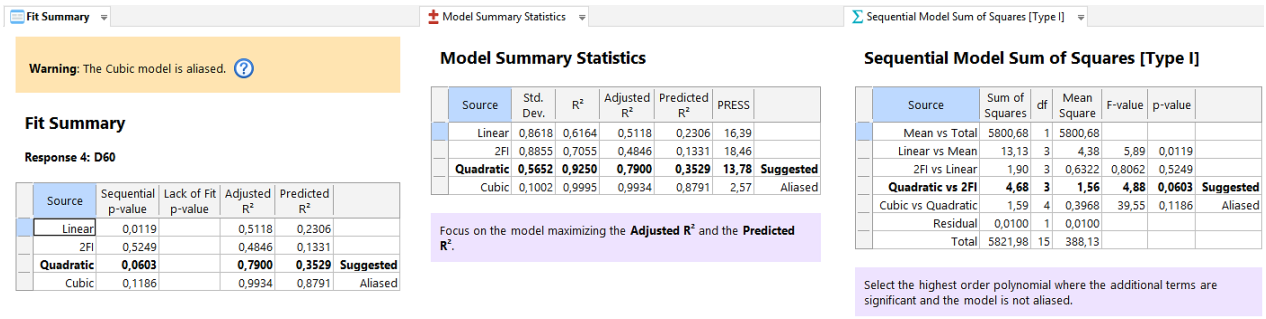

Fit Summary | Model Summary Statistics | Sequential Model Sum of Squares [Type I]

Warning: The Cubic model is aliased.

Fit Summary

Response 4: D60

Source	Sequential p-value	Lack of Fit p-value	Adjusted R^2	Predicted R^2	
Linear	0,0119		0,5118	0,2306	
2FI	0,5249		0,4846	0,1331	
Quadratic	**0,0603**		**0,7900**	**0,3529**	**Suggested**
Cubic	0,1186		0,9934	0,8791	Aliased

Model Summary Statistics

Source	Std. Dev.	R^2	Adjusted R^2	Predicted R^2	PRESS	
Linear	0,8618	0,6164	0,5118	0,2306	16,39	
2FI	0,8855	0,7055	0,4846	0,1331	18,46	
Quadratic	**0,5652**	**0,9250**	**0,7900**	**0,3529**	**13,78**	**Suggested**
Cubic	0,1002	0,9995	0,9934	0,8791	2,57	Aliased

Focus on the model maximizing the **Adjusted R^2** and the **Predicted R^2**.

Sequential Model Sum of Squares [Type I]

Source	Sum of Squares	df	Mean Square	F-value	p-value	
Mean vs Total	5800,68	1	5800,68			
Linear vs Mean	13,13	3	4,38	5,89	0,0119	
2FI vs Linear	1,90	3	0,6322	0,8062	0,5249	
Quadratic vs 2FI	**4,68**	**3**	**1,56**	**4,88**	**0,0603**	**Suggested**
Cubic vs Quadratic	1,59	4	0,3968	39,55	0,1186	Aliased
Residual	0,0100	1	0,0100			
Total	5821,98	15	388,13			

Select the highest order polynomial where the additional terms are significant and the model is not aliased.

Figure 16. Preliminary information given by the software for modelling the D60

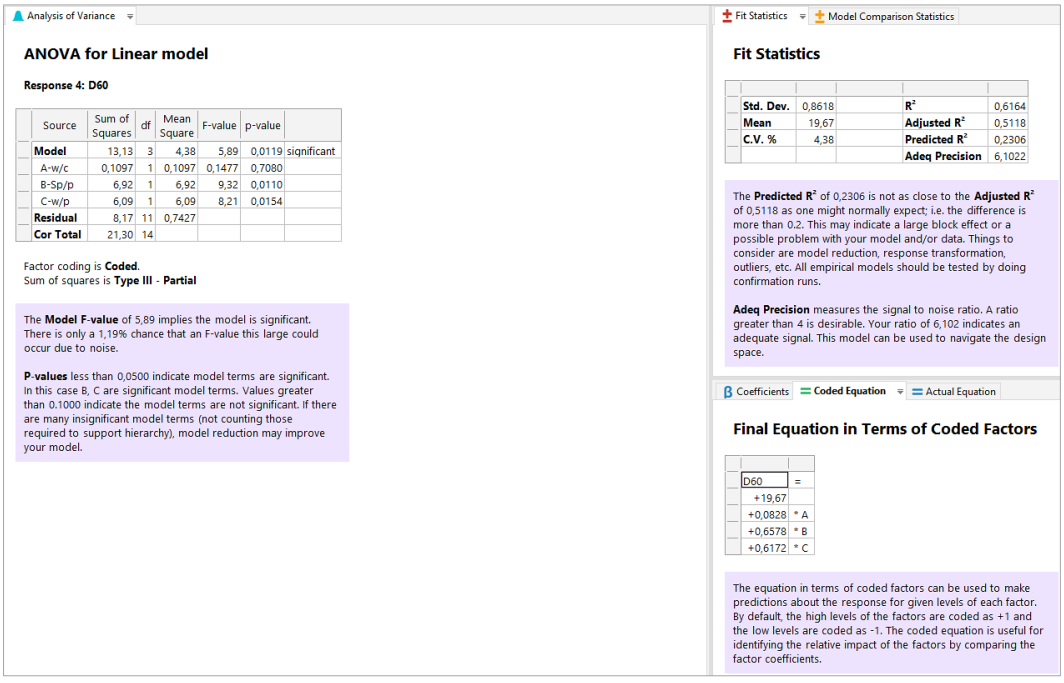

Analysis of Variance | Fit Statistics | Model Comparison Statistics

ANOVA for Linear model

Response 4: D60

Source	Sum of Squares	df	Mean Square	F-value	p-value	
Model	13,13	3	4,38	5,89	0,0119	significant
A-w/c	0,1097	1	0,1097	0,1477	0,7080	
B-Sp/p	6,92	1	6,92	9,32	0,0110	
C-w/p	6,09	1	6,09	8,21	0,0154	
Residual	8,17	11	0,7427			
Cor Total	21,30	14				

Factor coding is **Coded**.
Sum of squares is **Type III - Partial**

The **Model F-value** of 5,89 implies the model is significant. There is only a 1,19% chance that an F-value this large could occur due to noise.

P-values less than 0,0500 indicate model terms are significant. In this case B, C are significant model terms. Values greater than 0.1000 indicate the model terms are not significant. If there are many insignificant model terms (not counting those required to support hierarchy), model reduction may improve your model.

Fit Statistics

Std. Dev.	0,8618	**R^2**	0,6164
Mean	19,67	**Adjusted R^2**	0,5118
C.V. %	4,38	**Predicted R^2**	0,2306
		Adeq Precision	6,1022

The **Predicted R^2** of 0,2306 is not as close to the **Adjusted R^2** of 0,5118 as one might normally expect; i.e. the difference is more than 0.2. This may indicate a large block effect or a possible problem with your model and/or data. Things to consider are model reduction, response transformation, outliers, etc. All empirical models should be tested by doing confirmation runs.

Adeq Precision measures the signal to noise ratio. A ratio greater than 4 is desirable. Your ratio of 6,102 indicates an adequate signal. This model can be used to navigate the design space.

Coefficients | Coded Equation | Actual Equation

Final Equation in Terms of Coded Factors

D60	=
+19,67	
+0,0828	* A
+0,6578	* B
+0,6172	* C

The equation in terms of coded factors can be used to make predictions about the response for given levels of each factor. By default, the high levels of the factors are coded as +1 and the low levels are coded as -1. The coded equation is useful for identifying the relative impact of the factors by comparing the factor coefficients.

Figure 17. Analysis of Variance and statistics data and comments for the quadratic model applied to the D60

4.4. Summary of the Response Models

The software provides a summary of all the models created, which is presented in Table 4. As previously noted, similarities are observed between the models for t0 and t60, as well as between those for D0 and D60. The significant terms and the magnitude of their corresponding coefficients are similar. This was an expected finding since t0 and t60, as well as D0 and D60, represent the same properties measured at different ages, respectively.

Table 4. Summary of the significant terms of the response models

	Intercept	A	B	C	AB	AC	BC	A^2	B^2	C^2
t0	72.4867	-2.05125	-2.47125	-8.475	0.285	-0.23	-0.2075	2.14708	0.281667	-0.307083
p-values		0.0086	0.0039	<0.0001	0.6975	0.7531	0.7764	0.0147	0.6522	0.6239
D0	20.23	0.278125	0.44375	0.428125	-0.2	0.25625	0.69375			
p-values		0.1258	0.0260	0.0301	0.4102	0.2979	0.0167			
$1/\sqrt{t60}$	0.0988192	0.00300114	0.0055691	0.00755337						
p-values		0.0011	<0.0001	<0.0001						
D60	19.665	0.0882125	0.657812	0.617187						
p-values		0.7080	0.0110	0.0154						

p-value shading: $p<0.05$; $0.05\leq p<0.1$; $p\geq 0.1$.

From the experimental results and modelling, several trends are observed. For slump flow, the increase in the Sp/p ratio enhances particle dispersion through electrostatic and steric effects, which reduces yield stress and promotes higher flowability. However, the excessive increase in the w/c ratio leads to segregation tendencies, reflecting the trade-off between fluidity and stability, a phenomenon widely reported in recent studies on SCC and printable concretes [21, 48]. For Marsh funnel time, the results demonstrate that viscosity is controlled not only by the absolute water content but also by the balance between powder concentration and dispersant efficiency. This explains the nonlinear trend where moderate w/c ratios decrease viscosity, but higher values increase flow time due to dilution and flocculation effects. Such interactions confirm the necessity of using CCD rather than simpler DOE methods.

The predictive models link the residual patterns to the adequacy of the quadratic form. The ability of the models to reproduce nonlinear behaviors supports their theoretical robustness. Moreover, the optimized region identified in this study is consistent with prior observations in UHPC and SCC optimization research [46, 47], which validates the broader applicability of our approach. Beyond the statistical fit, these results have practical implications: they provide mix designers with a reliable tool to anticipate the rheological response of pastes before scaling up to mortar or concrete. This reduces experimental workload and supports more sustainable practices by minimizing material waste during trial-and-error testing.

4.5. Prediction of Results Based on Response Models

One of the great advantages of conducting DOE is the ability to develop response models and subsequently predict results. Once the response models are established, it becomes possible to predict values of t0, D0, t60, and D60 for any mix composition with input parameters close to the tested range. Figure 18 illustrates this prediction in the software, showing predicted results of t0 = 75.9 s, D0 = 20.0 cm, t60 = 107.3 s, and D60 = 19.7 cm for a composition with input parameters w/c = 0.285, Sp/p = 0.85, and w/p = 0.52. The software also provides confidence intervals with 90% confidence.

4.6. Mix Composition Optimization Based on Response Models

Even more interesting—and perhaps the greatest advantage of using DOE compared to the trial-and-error methodology—is the ability to find an optimized mix composition through response models. The user can specify which variables should be maximized or minimized, set upper and lower limits, define target values, and assign relative importance or weights to determine the overall 'Desirability.' Figure 19 shows an example of the optimization process, with the software providing the optimized solution. Additionally, Figures 20 and 21 present graphical explanations of the process and illustrate how 'Desirability' is determined.

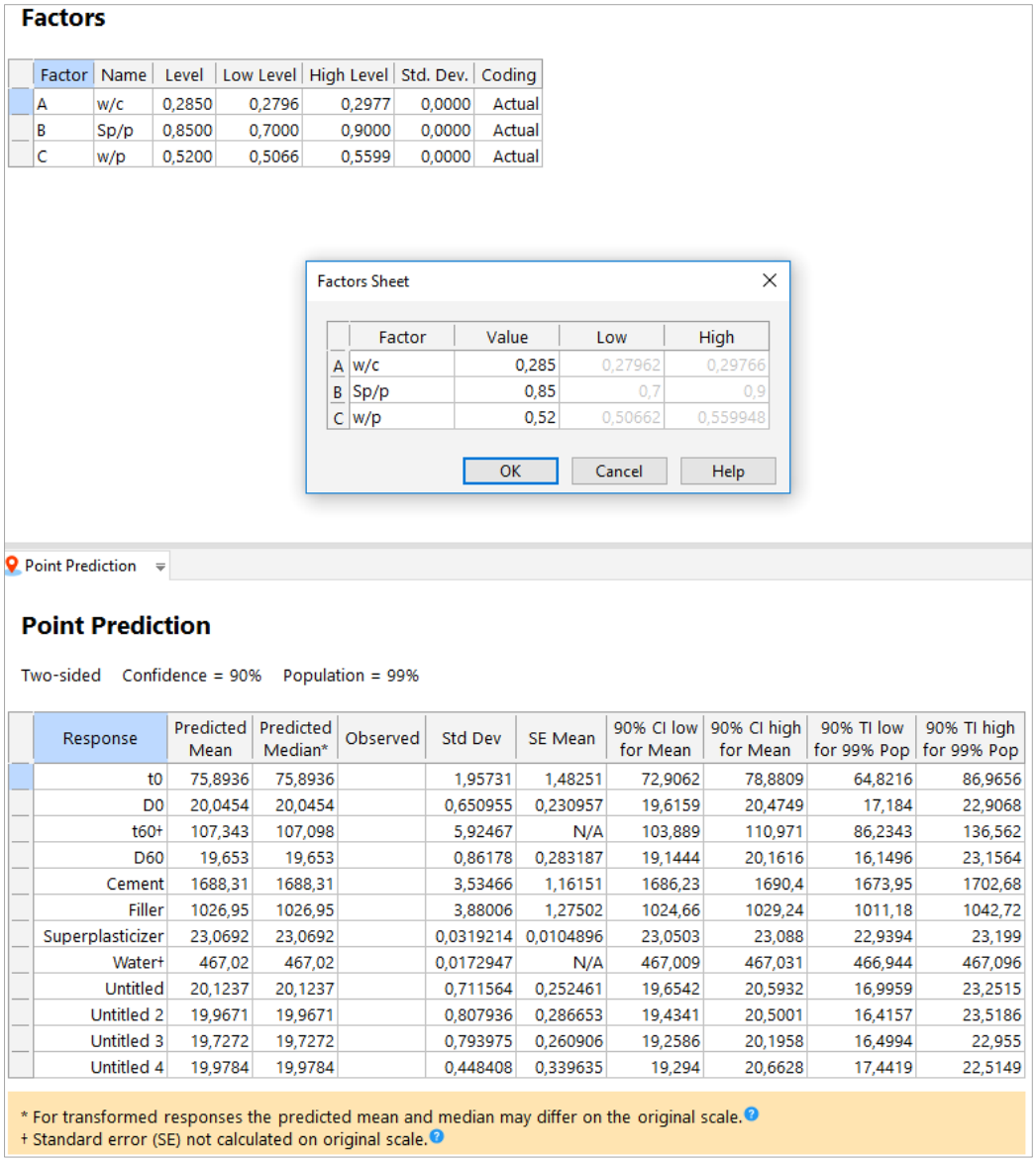

Factors

	Factor	Name	Level	Low Level	High Level	Std. Dev.	Coding
	A	w/c	0,2850	0,2796	0,2977	0,0000	Actual
	B	Sp/p	0,8500	0,7000	0,9000	0,0000	Actual
	C	w/p	0,5200	0,5066	0,5599	0,0000	Actual

Factors Sheet

	Factor	Value	Low	High
A	w/c	0,285	0,27962	0,29766
B	Sp/p	0,85	0,7	0,9
C	w/p	0,52	0,50662	0,559948

OK Cancel Help

Point Prediction

Point Prediction

Two-sided Confidence = 90% Population = 99%

	Response	Predicted Mean	Predicted Median*	Observed	Std Dev	SE Mean	90% CI low for Mean	90% CI high for Mean	90% TI low for 99% Pop	90% TI high for 99% Pop
	t0	75,8936	75,8936		1,95731	1,48251	72,9062	78,8809	64,8216	86,9656
	D0	20,0454	20,0454		0,650955	0,230957	19,6159	20,4749	17,184	22,9068
	t60+	107,343	107,098		5,92467	N/A	103,889	110,971	86,2343	136,562
	D60	19,653	19,653		0,86178	0,283187	19,1444	20,1616	16,1496	23,1564
	Cement	1688,31	1688,31		3,53466	1,16151	1686,23	1690,4	1673,95	1702,68
	Filler	1026,95	1026,95		3,88006	1,27502	1024,66	1029,24	1011,18	1042,72
	Superplasticizer	23,0692	23,0692		0,0319214	0,0104896	23,0503	23,088	22,9394	23,199
	Water+	467,02	467,02		0,0172947	N/A	467,009	467,031	466,944	467,096
	Untitled	20,1237	20,1237		0,711564	0,252461	19,6542	20,5932	16,9959	23,2515
	Untitled 2	19,9671	19,9671		0,807936	0,286653	19,4341	20,5001	16,4157	23,5186
	Untitled 3	19,7272	19,7272		0,793975	0,260906	19,2586	20,1958	16,4994	22,955
	Untitled 4	19,9784	19,9784		0,448408	0,339635	19,294	20,6628	17,4419	22,5149

* For transformed responses the predicted mean and median may differ on the original scale.
+ Standard error (SE) not calculated on original scale.

Figure 18. Response prediction for the mix composition with w/c=0.285, Sp/p=0.85 and w/p=0.52

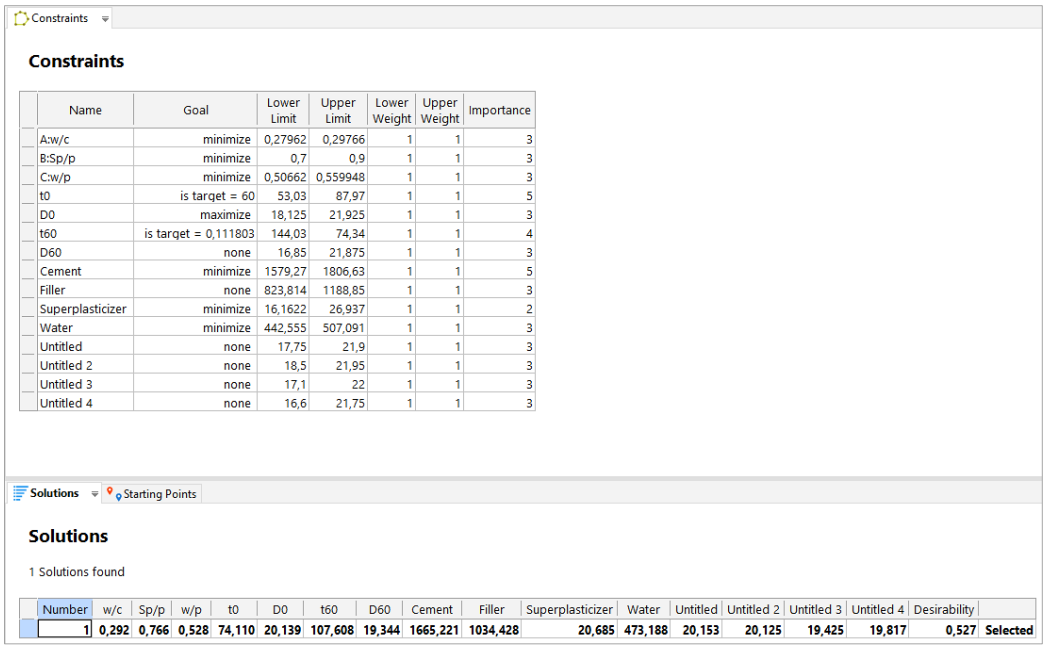

Constraints

Constraints

	Name	Goal	Lower Limit	Upper Limit	Lower Weight	Upper Weight	Importance
	A:w/c	minimize	0,27962	0,29766	1	1	3
	B:Sp/p	minimize	0,7	0,9	1	1	3
	C:w/p	minimize	0,50662	0,559948	1	1	3
	t0	is target = 60	53,03	87,97	1	1	5
	D0	maximize	18,125	21,925	1	1	3
	t60	is target = 0,111803	144,03	74,34	1	1	4
	D60	none	16,85	21,875	1	1	3
	Cement	minimize	1579,27	1806,63	1	1	5
	Filler	none	823,814	1188,85	1	1	3
	Superplasticizer	minimize	16,1622	26,937	1	1	2
	Water	minimize	442,555	507,091	1	1	3
	Untitled	none	17,75	21,9	1	1	3
	Untitled 2	none	18,5	21,95	1	1	3
	Untitled 3	none	17,1	22	1	1	3
	Untitled 4	none	16,6	21,75	1	1	3

Solutions Starting Points

Solutions

1 Solutions found

Number	w/c	Sp/p	w/p	t0	D0	t60	D60	Cement	Filler	Superplasticizer	Water	Untitled	Untitled 2	Untitled 3	Untitled 4	Desirability	
1	0,292	0,766	0,528	74,110	20,139	107,608	19,344	1665,221	1034,428	20,685	473,188	20,153	20,125	19,425	19,817	0,527	Selected

Figure 19. Constraints and solutions of the optimized composition

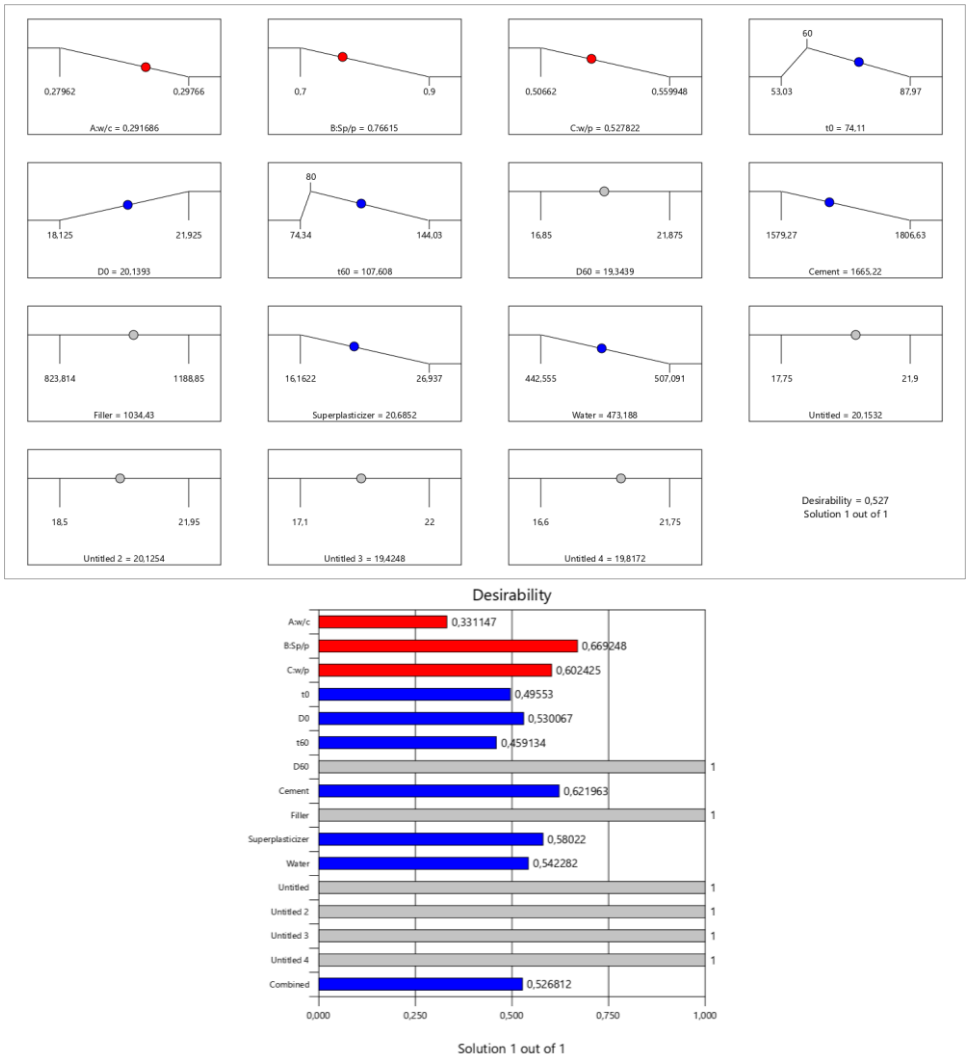

Figure 20. Explanation of the 'Desirability' of the solution: a) for each constraint individually, and b) comparison between constraints

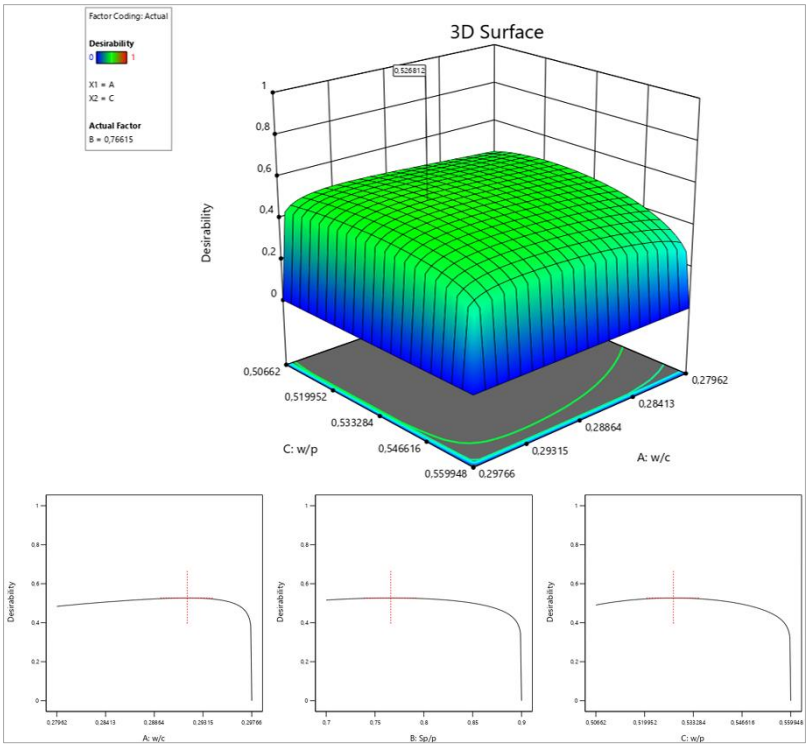

Figure 21. Optimization of the 'Desirability' – graphical view

5. Evaluation of the central composite design approach

Similarly to Part I of this research, this section reflects on the methodology applied and compares it with more conventional approaches. In this study, the DOE was based on a Central Composite Design (CCD), in which input parameters were varied simultaneously to assess their combined influence on the fresh properties of cement-based pastes. The following summarizes the main advantages and disadvantages of this approach compared with the trial-and-error method used in Part I.

Advantages of the central composite design approach:

- Complex systems with multiple interacting factors can be investigated with a reduced number of experiments;
- Response models provide a scientifically grounded understanding of parameter effects;
- The models capture not only primary effects but also two-factor interactions and quadratic (or higher-order) effects;
- Software tools assist users by generating graphs and statistical analyses;
- The models enable prediction of results for compositions not directly tested;
- Optimized mix designs can be obtained systematically.

Disadvantages of the central composite design approach:

- The number of input parameters must be limited and well defined, and the models are most reliable within these boundaries;
- Preliminary trial-and-error tests are often required to establish feasible parameter ranges before outlining the DOE;
- Intermediate results are often not interpretable until the full design is completed;
- Without dedicated software, CCD is difficult to implement effectively;
- The interpretation of model outputs can be challenging for non-specialists;
- Developing and analyzing the response models is essential for extracting meaningful conclusions.

The traditional approach uses a combination of scientific intuition and design of experiments (DOE) methods to choose which candidates to test. In both cases, resource-intensive experiments are needed to validate results. While the present study demonstrates the clear benefits of CCD over traditional trial-and-error strategies in terms of efficiency and predictive capability, it is important to note that these approaches should not be viewed as mutually exclusive. In practice, hybrid strategies are increasingly adopted, where empirical knowledge and preliminary trial-and-error tests provide a practical starting point, while CCD or other DOE methodologies refine the process by capturing nonlinear and interaction effects. This combination enables practitioners to benefit from the intuitive simplicity of conventional methods while exploiting the statistical rigor of CCD. As such, CCD should be regarded as a complementary and enhancing tool rather than a strict replacement, strengthening both the reliability of mix design and the transferability of laboratory findings to real-world applications.

6. Conclusions

Fresh properties of cement-based pastes were characterized using different experimental approaches. This paper relates to the research in which the DOE was planned based on a central composite design. From this paper and the overall research work, the following conclusions are drawn:

- The water-to-powder ratio has the strongest effect on the overall workability of the pastes – the higher the water-to-powder ratio, the higher the workability. This effect is especially observed in the Marsh funnel test when carried out immediately after mixing, where the influence of the water-to-powder ratio on changes in flow time is greater than the combined influence of the superplasticizer-to-powder ratio and the water-to-powder ratio.
- The superplasticizer-to-powder ratio has the second highest effect on the overall workability of the pastes – the higher the superplasticizer-to-powder ratio, the higher the workability. The effect of the superplasticizer-to-powder ratio is much more pronounced in the mini-cone slump test than in the Marsh funnel test.
- The response models show that the influence of the input parameters on workability measured immediately after mixing cannot be explained solely by linear correlations. Interaction effects and second-order effects are detected in the response models. The interaction effects of the input parameters account for about 50% of the effects on changes in the flow diameter. The interaction and second-order effects on changes in flow time in the Marsh funnel test accounts for about 20%.

- A DOE based on a central composite design approach is suitable for in-depth research where advanced statistical analysis and modeling are required. However, specialized software is necessary to assist the user when applying a DOE based on a central composite design.
- When the purpose is simply to recognize principal trends or clarify uncertainties over a wide range of a single input variable, basic approaches are more appropriate (e.g., trial-and-error experiments or varying the input variable by increments).

Sometimes, a combination of different approaches might be the best solution: using basic methods to understand primary effects and then defining a central composite design DOE for more detailed analysis.

7. Declarations

7.1. Data Availability Statement

The data presented in this study are available on request from the corresponding author.

7.2. Funding and Acknowledgments

This work was financially supported by: UID/04708/2025 and https://doi.org/10.54499/UID/04708/2025, of the CONSTRUCT - Instituto de I&D em Estruturas e Construções - funded by Fundação para a Ciência e a Tecnologia, I.P./ MECI, through the national funds.

7.3. Conflicts of Interest

The author declares no conflict of interest.

8. References

[1] Okamura, H., & Ouchi, M. (2003). Self-compacting concrete. Journal of Advanced Concrete Technology, 1(1), 5-15. doi:.10.3151/jact.1.5

[2] Khayat, K. H. (1999). Workability, testing, and performance of self-consolidating concrete. Materials Journal, 96(3), 346-353. doi:10.14359/632.

[3] Richard, P., & Cheyrezy, M. (1995). Composition of reactive powder concretes. Cement and Concrete Research, 25(7), 1501–1511. doi:10.1016/0008-8846(95)00144-2.

[4] Mehta, P. K., & Monteiro, P. J. (2006). Concrete microstructure, properties, and materials. McGraw-Hill, New York, United States.

[5] Domone, P. (1998). The slump flow test for high-workability concrete. Cement and Concrete Research, 28(2), 177–182. doi:10.1016/S0008-8846(97)00224-X.

[6] Roussel, N., & Le Roy, R. (2005). The Marsh cone: A test or a rheological apparatus? Cement and Concrete Research, 35(5), 823–830. doi:10.1016/j.cemconres.2004.08.019.

[7] Roussel, N., Stefani, C., & Leroy, R. (2005). From mini-cone test to Abrams cone test: Measurement of cement-based materials yield stress using slump tests. Cement and Concrete Research, 35(5), 817–822. doi:10.1016/j.cemconres.2004.07.032.

[8] Roussel, N., & Coussot, P. (2005). "Fifty-cent rheometer" for yield stress measurements: From slump to spreading flow. Journal of Rheology, 49(3), 705–718. doi:10.1122/1.1879041.

[9] Saak, A. W., Jennings, H. M., & Shah, S. P. (2001). The influence of wall slip on yield stress and viscoelastic measurements of cement paste. Cement and Concrete Research, 31(2), 205–212. doi:10.1016/S0008-8846(00)00440-3.

[10] Wallevik, J. E. (2006). Relationship between the Bingham parameters and slump. Cement and Concrete Research, 36(7), 1214–1221. doi:10.1016/j.cemconres.2006.03.001.

[11] Wallevik, O. H., Feys, D., Wallevik, J. E., & Khayat, K. H. (2015). Avoiding inaccurate interpretations of rheological measurements for cement-based materials. Cement and Concrete Research, 78, 100–109. doi:10.1016/j.cemconres.2015.05.003.

[12] Guria, C., Kumar, R., & Mishra, P. (2013). Rheological analysis of drilling fluid using Marsh Funnel. Journal of Petroleum Science and Engineering, 105, 62–69. doi:10.1016/j.petrol.2013.03.027.

[13] Ghezal, A., & Khayat, K. H. (2002). Optimizing self-consolidating concrete with limestone filler by using statistical factorial design methods. Materials Journal, 99(3), 264-272. doi:10.14359/11972.

[14] Rezaifar, O., Hasanzadeh, M., & Gholhaki, M. (2016). Concrete made with hybrid blends of crumb rubber and metakaolin: Optimization using Response Surface Method. Construction and Building Materials, 123, 59–68. doi:10.1016/j.conbuildmat.2016.06.047.

[15] Aziminezhad, M., Mohamedelhassan, E., & Mahdikhani, M. (2024). Multi-property response and optimisation of lightweight self-consolidating mortar containing silica fume and nano silica. European Journal of Environmental and Civil Engineering, 28(5), 1163-1182. doi:10.1080/19648189.2023.2245863.

[16] Box, G. E. P., & Wilson, K. B. (1951). On the Experimental Attainment of Optimum Conditions. Journal of the Royal Statistical Society Series B: Statistical Methodology, 13(1), 1–38. doi:10.1111/j.2517-6161.1951.tb00067.x.

[17] Montgomery, D. C. (2017). Design and analysis of experiments. John Wiley & Sons, Hoboken, United States.

[18] Myers, R. H., Montgomery, D. C., & Anderson-Cook, C. M. (2016). Response surface methodology: process and product optimization using designed experiments. John Wiley & Sons, Hoboken, United States.

[19] Fan, D., Lu, J. X., Liu, K., Ban, J., Yu, R., & Poon, C. S. (2024). Multi-scale design of ultra-high performance concrete (UHPC) composites with centroplasm theory. Composites Part B: Engineering, 281, 111562. doi:10.1016/j.compositesb.2024.111562.

[20] Hou, D., Zhang, X., Zhang, K., Zhang, X., Bao, M., Jin, L., ... & Wang, X. (2025). Optimizing lightweight UHPC through the synergy of lightweight aggregate, filler, and polymer fiber via response surface methodology. Construction and Building Materials, 463, 140104. doi:10.1016/j.conbuildmat.2025.140104.

[21] Hayek, M., El Bitouri, Y., Bouarab, K., & Yahia, A. (2025). Structural Build-Up of Cement Pastes: A Comprehensive Overview and Key Research Directions. Construction Materials, 5(2), 31. doi:10.3390/constrmater5020031.

[22] Rojo-López, G., Nunes, S., González-Fonteboa, B., & Martínez-Abella, F. (2020). Quaternary blends of portland cement, metakaolin, biomass ash and granite powder for production of self-compacting concrete. Journal of Cleaner Production, 266, 121666. doi:10.1016/j.jclepro.2020.121666.

[23] Hu, C. (1995). Rheology of fluid concretes. Ph.D. Thesis, Ecole Nationale des Ponts et Chaussées, Champs-sur-Marne, France.

[24] Juvas, K., Kappi, A., Salo, K., & Nordenswan, E. (2001). The effects of cement variations on concrete workability. Nordic Concrete Research-Publications, 26, 39–46.

[25] Nunes, S., Figueiras, H., Milheiro Oliveira, P., Coutinho, J. S., & Figueiras, J. (2006). A methodology to assess robustness of SCC mixtures. Cement and Concrete Research, 36(12), 2115–2122. doi:10.1016/j.cemconres.2006.10.003.

[26] Nunes, S., Oliveira, P. M., Coutinho, J. S., & Figueiras, J. (2009). Interaction diagrams to assess SCC mortars for different cement types. Construction and Building Materials, 23(3), 1401–1412. doi:10.1016/j.conbuildmat.2008.07.009.

[27] Xu, K., Yang, J., He, H., Wei, J., & Zhu, Y. (2025). Influences of Additives on the Rheological Properties of Cement Composites: A Review of Material Impacts. Materials, 18(8), 1753. doi:10.3390/ma18081753.

[28] Matos, A. M., Maia, L., Nunes, S., & Milheiro-Oliveira, P. (2018). Design of self-compacting high-performance concrete: Study of mortar phase. Construction and Building Materials, 167, 617–630. doi:10.1016/j.conbuildmat.2018.02.053.

[29] Maia, L., & Neves, D. (2017). Developing a Commercial Self-Compacting Concrete without Limestone Filler and With Volcanic Aggregate Materials. Procedia Structural Integrity, 5, 147–154. doi:10.1016/j.prostr.2017.07.085.

[30] Uysal, M., & Tanyildizi, H. (2011). Predicting the core compressive strength of self-compacting concrete (SCC) mixtures with mineral additives using artificial neural network. Construction and Building Materials, 25(11), 4105–4111. doi:10.1016/j.conbuildmat.2010.11.108.

[31] Richards, J. A., Li, H., O'Neill, R. E., Laidlaw, F. H. J., & Royer, J. R. (2024). Fresh cement as a frictional non-Brownian suspension. Powder Technology, 441, 119791. doi:10.1016/j.powtec.2024.119791.

[32] Yan, K., & Shi, C. (2010). Prediction of elastic modulus of normal and high strength concrete by support vector machine. Construction and Building Materials, 24(8), 1479–1485. doi:10.1016/j.conbuildmat.2010.01.006.

[33] Kabiru, O. A., Owolabi, T. O., Ssennoga, T., & Olatunji, S. O. (2014). Performance comparison of SVM and ANN in predicting compressive strength of concrete. IOSR Journal of Computer Engineering, 16(5), 88–94.

[34] Azimi-Pour, M., Eskandari-Naddaf, H., & Pakzad, A. (2020). Linear and non-linear SVM prediction for fresh properties and compressive strength of high volume fly ash self-compacting concrete. Construction and Building Materials, 230, 117021. doi:10.1016/j.conbuildmat.2019.117021.

[35] Abd, A. M., & Abd, S. M. (2017). Modelling the strength of lightweight foamed concrete using support vector machine (SVM). Case Studies in Construction Materials, 6, 8–15. doi:10.1016/j.cscm.2016.11.002.

[36] Pinheiro, C., Rios, S., Viana da Fonseca, A., Fernández-Jiménez, A., & Cristelo, N. (2020). Application of the response surface method to optimize alkali activated cements based on low-reactivity ladle furnace slag. Construction and Building Materials, 264, 120271. doi:10.1016/j.conbuildmat.2020.120271.

[37] Khuri, A. I., & Mukhopadhyay, S. (2010). Response surface methodology. WIREs Computational Statistics, 2(2), 128–149. doi:10.1002/wics.73.

[38] Myers, R. H., Khuri, A. I., Carter, W. H., & Khuri, A. I. (1989). Response Surface Methodology: 1966-1988. Technometrics, 31(2), 137. doi:10.2307/1268813.

[39] Bezerra, M. A., Santelli, R. E., Oliveira, E. P., Villar, L. S., & Escaleira, L. A. (2008). Response surface methodology (RSM) as a tool for optimization in analytical chemistry. Talanta, 76(5), 965–977. doi:10.1016/j.talanta.2008.05.019.

[40] Lamidi, S., Olaleye, N., Bankole, Y., Obalola, A., Aribike, E., & Adigun, I. (2022). Applications of response surface methodology (RSM) in product design, development, and process optimization. IntechOpen, London, United Kingdom. doi:10.5772/intechopen.106763.

[41] Ali, M., Kumar, A., Yvaz, A., & Salah, B. (2023). Central composite design application in the optimization of the effect of pumice stone on lightweight concrete properties using RSM. Case Studies in Construction Materials, 18, e01958. doi:10.1016/j.cscm.2023.e01958.

[42] Box, G. E., Hunter, J. S., & Hunter, W. G. (2005). Statistics for experimenters: design, innovation, and discovery. John Wiley & Sons, Hoboken, United States.

[43] Taguchi, G. (1987). System of experimental design; engineering methods to optimize quality and minimize costs. UNIPUB/Kaus International, New York, United States.

[44] Plackett, R. L., & Burman, J. P. (1946). The Design of Optimum Multifactorial Experiments. Biometrika, 33(4), 305. doi:10.2307/2332195.

[45] Koshal, J., Nedić, A., & Shanbhag, U. V. (2011). Multiuser optimization: Distributed algorithms and error analysis. SIAM Journal on Optimization, 21(3), 1046-1081. doi:10.1137/090770102.

[46] Yu, R., Spiesz, P., & Brouwers, H. J. H. (2014). Effect of nano-silica on the hydration and microstructure development of Ultra-High Performance Concrete (UHPC) with a low binder amount. Construction and Building Materials, 65, 140-150. doi:10.1016/j.conbuildmat.2014.04.063.

[47] Rojo-López, G., Nunes, S., González-Fonteboa, B., & Martínez-Abella, F. (2020). Quaternary blends of portland cement, metakaolin, biomass ash and granite powder for production of self-compacting concrete. Journal of Cleaner Production, 266, 121666. doi:10.1016/j.jclepro.2020.121666.

[48] Sobuz, M. H. R., Aditto, F. S., Datta, S. D., Kabbo, M. K. I., Jabin, J. A., Hasan, N. M. S., ... & Zaman, A. A. U. (2024). High-strength self-compacting concrete production incorporating supplementary cementitious materials: experimental evaluations and machine learning modelling. International Journal of Concrete Structures and Materials, 18(1), 67. doi:10.1186/s40069-024-00707-7.

[49] EN 196:1995. (1995). EN 196-1: Methods of testing cement — Part 1: Determination of strength. European Committee for Standardization (CEN), Brussels, Belgium.

[50] EN 445:2007. (2007). Grout for prestressing tendons - Test methods. European Committee for Standardization (CEN), Brussels, Belgium.

[51] Stat-Ease. (2019). Design-Expert® Software User's Guide (v7/v13). Stat-Ease, Minneapolis, United States.